Physical Properties of Wolf-Rayet Stars

Paul A. Crowther

Department of Physics & Astronomy, University of Sheffield, Hounsfield Road, Sheffield, S3 7RH, United Kingdom, email: Paul.Crowther@sheffield.ac.uk

Key Words stars: Wolf-Rayet; stars: fundamental parameters; stars: evolution; stars: abundances

Abstract The striking broad emission line spectroscopic appearance of Wolf-Rayet (WR) stars has long defied analysis, due to the extreme physical conditions within their line and continuum forming regions. Recently, model atmosphere studies have advanced sufficiently to enable the determination of stellar temperatures, luminosities, abundances, ionizing fluxes and wind properties. The observed distributions of nitrogen (WN) and carbon (WC) sequence WR stars in the Milky Way and in nearby star forming galaxies are discussed; these imply lower limits to progenitor masses of ∼25, 40, 75 $M_\odot$ for hydrogen-depleted (He-burning) WN, WC, and H-rich (H-burning) WN stars, respectively. WR stars in massive star binaries permit studies of wind-wind interactions and dust formation in WC systems. They also show that WR stars have typical masses of 10–25$M_\odot$, extending up to 80$M_\odot$ for H-rich WN stars. Theoretical and observational evidence that WR winds depend on metallicity is presented, with implications for evolutionary models, ionizing fluxes, and the role of WR stars within the context of core-collapse supernovae and long-duration gamma ray bursts.

CONTENTS

1 Introduction

Massive stars dominate the feedback to the local interstellar medium (ISM) in star-forming galaxies via their stellar winds and ultimate death as core-collapse supernovae. In particular, Wolf-Rayet (WR) stars typically have wind densities an order of magnitude higher than massive O stars. They contribute to the chemical enrichment of galaxies, they are the prime candidates for the immediate progenitors of long, soft Gamma Ray Bursts (GRBs, Woosley & Bloom 2006), and they provide a signature of high-mass star formation in galaxies (Schaerer & Vacca 1998).

Spectroscopically, WR stars are spectacular in appearance, with strong, broad emission lines instead of the narrow absorption lines which are typical of normal stellar populations (e.g. Beals 1940). The class are named after Wolf & Rayet (1867) who identified three stars in Cygnus with such broad emission lines. It was immediately apparent that their spectra came in two flavours, subsequently identified as those with strong lines of helium and nitrogen (WN subtypes) and those with strong helium, carbon, and oxygen (WC and WO subtypes). Gamov (1943) first suggested that the anomalous composition of WR stars was the result of nuclear processed material being visible on their surfaces, although this was not universally established until the final decade of the 20th Century (Lamers et al. 1991). Specifically, WN and WC stars show the products of the CNO cycle (H-burning) and the triple-α (He-burning), respectively. In reality, there is a continuity of physical and chemical properties between O supergiants and WN

subtypes.

Typically, WR stars have masses of 10–25 $M_{\odot}$, and are descended from O-type stars. They spend ∼10% of their ∼5Myr lifetime as WR stars (Meynet & Maeder 2005). At Solar metallicity the minimum initial mass for a star to become a WR star is ∼25 $M_{\odot}$. This corresponds closely to the Humphreys & Davidson (1979) limit for red supergiants (RSG), according to a comparison between the current temperature calibration of RSG and stellar models that allow for mass-loss and rotation (e.g. Levesque et al. 2005). Consequently, some single WR stars are post-red supergiants within a fairly limited mass range of probably 25–30$M_{\odot}$. Evolution proceeds via an intermediate Luminous Blue Variable (LBV) phase above 30$M_{\odot}$. For close binaries, the critical mass for production of a WR star has no such robust lower limit, since Roche lobe overflow or common envelope evolution could produce a WR star instead of an extended RSG phase.

The strong, broad emission lines seen in spectra of WR stars are due to their powerful stellar winds. The wind is sufficiently dense that an optical depth of unity in the continuum arises in the outflowing material. The spectral features are formed far out in the wind and are seen primarily in emission. The line and continuum formation regions are geometrically extended compared to the stellar radii and their physical depths are highly wavelength dependent. The unique spectroscopic signature of WR stars has permitted their detection individually in Local Group galaxies (e.g. Massey & Johnson 1998; Massey 2003), collectively within knots of local star forming galaxies (e.g. Hadfield & Crowther 2006), and as significant contributors to the average rest-frame UV spectrum of Lyman Break Galaxies (Shapley et al. 2003).

The present review focuses on observational properties of classical Wolf-Rayet

stars in the Milky Way and beyond, plus physical and chemical properties determined from spectroscopic analysis, plus comparisons with interior evolutionary models, and provides revisions to the topic with respect to the excellent Abbott & Conti (1987) review. Low mass ($\sim 0.6 M_{\odot}$) central stars of Planetary Nebulae displaying a Wolf-Rayet spectroscopic appearance (denoted [WR]) are not considered. Nevertheless, analysis tools discussed here are common to both types of star (e.g. Crowther et al. 2006a).

2 Observed Properties

2.1 Spectral Properties and Spectral Classification

Visual spectral classification of WR stars is based on emission line strengths and line ratios following Smith (1968a). WN spectral subtypes follow a scheme involving line ratios of N III-V and He I-II, ranging from WN2 to WN5 for 'early WN' (WNE) stars, and WN7 to WN9 for 'late WN' (WNL) stars, with WN6 stars either early or late-type. A 'h' suffix may be used to indicate the presence of emission lines due to hydrogen (Smith, Shara & Moffat 1996).

Complications arise for WN stars with intrinsically weak emission lines. For example, WR24 (WN6ha) has a He II λ4686 emission equivalent width that is an order of magnitude smaller than those in some other WN6 stars; the 'ha' nomenclature indicates that hydrogen is seen both in absorption and emission. From a standard spectroscopic viewpoint, such stars possess mid to late WN spectral classifications. However, their appearance is rather more reminiscent of Of stars than classic WN stars, since there exists a continuity of properties between normal O stars and late-type WN stars. These stars are widely believed to be massive O stars with relatively strong stellar winds at a rather early evolutionary

stage. They are believed not to represent the more mature, classic He-burning WN stars.

Smith, Crowther & Prinja (1994) extended the WN sequence to very late WN10–11 subtypes in order to include a group of emission line stars originally classified as Ofpe/WN9 (Bohannan & Walborn 1989). WN11 subtypes closely resemble extreme early-type B supergiants except for the presence of He II λ4686 emission. A quantitative comparison of optical line strengths in Of and WNL stars is presented in figure 8 of Bohannan & Crowther (1999). R127 (WN11) in the Large Magellanic Cloud (LMC) was later identified as a LBV (Stahl et al. 1983), whilst a famous Galactic LBV, AG Car exhibited a WN11-type spectrum at visual minimum (Walborn 1990; Smith et al. 1994).

Various multi-dimensional classification systems have been proposed for WN stars; they generally involve line strengths or widths, such that strong/broad lined stars have been labelled WN-B (Hiltner & Schild 1966), WN-s (Hamann, Koesterke & Wessolowski 1993) or WNb (Smith, Shara & Moffat 1996). Of these, none have generally been adopted. From a physical perspective, strong- and weak-lined WN stars do form useful sub-divisions. Therefore we shall define weak (-w) and strong (-s) WN stars as those with He II λ5412 equivalent widths smaller than or larger than 40 Å. An obvious limitation of such an approach is that intrinsically strong-lined WN stars would be diluted by binary companions or nearby stars in spatially crowded regions and so might not be identified as such. WNE-w stars tend to exhibit triangular line profiles rather than the more typical Gaussian lines of WNE-s stars (Marchenko et al. 2004), since one observes material much closer to the stellar core that is being strongly accelerated.

WC spectral subtypes depend on the line ratios of C III and C IV lines along

with the appearance of O III-V, spanning WC4 to WC9 subtypes, for which WC4–6 stars are 'early' (WCE) and WC7–9 are 'late' (WCL). Rare, oxygen-rich WO stars form an extension of the WCE sequence, exhibiting strong O VI $\lambda\lambda$3811-34 emission (Kingsburgh, Barlow & Storey 1995). The most recent scheme involves WO1 to WO4 subtypes depending on the relative strength of O V-VI and C IV emission lines (Crowther, De Marco & Barlow 1998). Finally, C IV λ5801-12 appears unusually strong in an otherwise normal WN star in a few cases, leading to an intermediate WN/C classification (Conti & Massey 1989). WN/C stars are indeed considered to be at an intermediate evolutionary phase between the WN and WC stages.

Representative examples of WN and WC stars are presented in Figure 1. Various X-ray to mid-IR spectroscopic datasets of Galactic Wolf-Rayet stars are presented in Table 1, including extreme ultraviolet synthetic spectra from model atmospheres (Smith, Norris & Crowther 2002; Hamann & Gräfener 2004).

2.2 Absolute magnitudes

WR stars cannot be distinguished from normal hot stars using UBV photometry. Broad-band visual measurements overestimate the true continuum level in extreme cases by up to 1 magnitude, or more typically 0.5 mag for single early-type WR stars due to their strong emission-line spectra. Consequently, Westerlund (1966) introduced narrow-band *ubyr* filters that were specifically designed to minimize the effect of WR emission lines (although their effect cannot be entirely eliminated). These passbands were later refined by Smith (1968b) and by Massey (1984), such that most photometry of WR stars has used the *ubvr* filter system, which is compared to Johnson UBV filters in Fig. 1.

As with normal stars, *ubv* photometry permits a determination of the interstellar extinction, A_v. Let us adopt a typical ratio of total, A_V to selective, $E(B-V) = A_B - A_V$ extinction, $R_V = A_V/E(B-V) = 3.1$. Following Turner (1982), the broad-band and narrow-band optical indices for WR stars are then related by:

$$A_v \;\; = \;\; 4.12\, E_{b-v} = 3.40\, E_{B-V} = 1.11\, A_V$$

A direct determination of WR distances via stellar parallax is only possible for γ Vel (WC8+O) using *Hipparcos*, and even that remains controversial (Millour et al. 2007). Otherwise, cluster or association membership is used to provide an approximate absolute magnitude-spectral type calibration for Milky Way WR stars. The situation is much better for WR stars in the Magellanic Clouds, although not all subtypes are represented. Typical absolute magnitudes range from M_v = –3 mag at earlier subtypes to –6 mag for late subtypes, or exceptionally –7 mag for hydrogen-rich WN stars. The typical spread is $\pm$0.5 mag at individual subtypes.

2.3 Observed distribution

Conti (1976) first proposed that a massive O star may lose a significant amount of mass via stellar winds, revealing first the H-burning products at its surface, and subsequently the He-burning products. These evolutionary stages are spectroscopically identified with the WN and WC types. This general picture has since become known as the 'Conti scenario'. Such stars should be over-luminous for their mass, in accord with observations of WR stars in binary systems. Massey (2003) provides a more general overview of massive stars within Local Group galaxies.

2.3.1 WR stars in Milky Way Wolf-Rayet stars are located in or close to massive star forming regions within the Galactic disk. A catalogue is provided by van der Hucht (2001). A quarter of the known WR stars in the Milky Way reside within massive clusters at the Galactic centre or in Westerlund 1 (van der Hucht 2006). From membership of WR stars in open clusters, Schild & Maeder (1984) and Massey, DeGioia-Eastwood & Waterhouse (2001) investigated the initial masses of WR stars empirically. A revised compilation is provided in Crowther et al. (2006b).

Overall, hydrogen-rich WN stars (WNha) are observed in young, massive clusters; their main-sequence turn-off masses (based on Meynet et al. 1994 isochrones) suggest initial masses of $65 - 110 M_{\odot}$, and are believed to be core-H burning (Langer et al. 1994; Crowther et al. 1995a). Lower-mass progenitors of 40–50$M_{\odot}$ are suggested for classic mid-WN, late WC, and WO stars. Progenitors of some early WN stars appear to be less massive still, suggesting an initial-mass cutoff for WR stars at Solar metallicity around $25 M_{\odot}$.

From an evolutionary perspective, the absence of RSGs at high luminosity and presence of H-rich WN stars in young massive clusters suggests the following variation of the Conti scenario in the Milky Way, i.e. for stars initially more massive than $\sim 75 M_{\odot}$

$$O \rightarrow \mathrm{WN(H-rich)} \rightarrow \mathrm{LBV} \rightarrow \mathrm{WN(H-poor)} \rightarrow \mathrm{WC} \rightarrow \mathrm{SN\,Ic},$$

whereas for stars of initial mass from $\sim 40 - 75 M_{\odot}$,

$$O \rightarrow \mathrm{LBV} \rightarrow \mathrm{WN(H-poor)} \rightarrow \mathrm{WC} \rightarrow \mathrm{SN\,Ic},$$

and for stars of initial mass in the range 25–40$M_{\odot}$,

$$O \rightarrow \mathrm{LBV/RSG} \rightarrow \mathrm{WN(H-poor)} \rightarrow \mathrm{SN\,Ib}.$$

Indeed, the role of the LBV phase is not yet settled – it may be circumvented entirely in some cases; it may follow the RSG stage, or it may even dominate pre-WR mass-loss for the most massive stars (Langer et al. 1994; Smith & Owocki 2006). Conversely, the presence of dense, circumstellar shells around Type IIn SN indicates that some massive stars may even undergo core-collapse during the LBV phase (Smith et al. 2007). Remarkably few Milky Way clusters host both RSG and WR stars, with the notable exception of Westerlund 1 (Clark et al. 2005); this suggests that the mass range common to both populations is fairly narrow.

Although optical narrow-band surveys (see below) have proved very successful for identifying WR stars in the Solar neighbourhood, only a few hundred WR stars are known in the Milky Way, whilst many thousands are expected within the Galactic disk (van der Hucht 2001). Consequently, near-IR narrow-band imaging surveys together with spectroscopic follow-up may be considered for more extensive surveys to circumvent high interstellar extinction (Homeier et al. 2003). Limitations of IR emission-line surveys are that fluxes of near-IR lines are much weaker than those of optical lines, Also, no strong WR lines are common to all spectral types in the frequently used K band. An added complication is that some WC stars form dust which heavily dilutes emission line fluxes longward of the visual. Nevertheless, infrared surveys are presently underway to get an improved census of WR stars in the Milky Way. Alternatively, WR candidates may be identified from their near- to mid-IR colours, which, as in other early-type supergiants, are unusual due to strong free-free excess emission (Hadfield et al. 2007).

2.3.2 WR stars in the Local Group WR stars have typically been discovered via techniques sensitive to their unusually broad emission-line spectra, based on objective prism searches or interference filter imaging (see Massey 2003). Narrow-band interference filter techniques have been developed (e.g. Moffat, Seggewiss & Shara 1985; Massey, Armandroff & Conti 1986) that distinguish strong WR emission lines at He II λ4686 (WN stars) and C III λ4650 (WC stars) from the nearby continuum. Such techniques have been applied to regions of the Milky Way disk, the Magellanic Clouds and other nearby galaxies. An example of this approach is presented in Figure 2 for the spiral galaxy NGC 300 ($d \sim$ 2 Mpc). A wide-field image of NGC 300 is presented, with OB complex IV-V indicated, together with narrow-band images centred at λ4684 (He II 4686) and λ4781 (continuum). Several WR stars are seen in the difference (He II-continuum) image, including an apparently single WC4 star (Schild et al. 2003).

It is well established that the absolute number of WR stars and their subtype distribution are metallicity dependent. N(WR)/N(O)$\sim$0.15 in the relatively metal-rich Solar Neighbourhood (Conti et al. 1983; van der Hucht 2001), yet N(WR)/N(O)$\sim$0.01 in the metal-deficient SMC on the basis of only 12 WR stars (Massey, Olsen & Parker 2003) versus $\sim$1000 O stars (Evans et al. 2004). It is believed that the majority of Galactic WR stars are the result of single-star evolution, yet some stars (e.g. V444 Cyg) result from close binary evolution (Vanbeveren et al. 1998).

Similar relative numbers of WN to WC stars are observed in the Solar Neighbourhood (Hadfield et al. 2007). In contrast, WN stars exceed WC stars by a factor of $\sim$5 and $\sim$10 for the LMC and SMC, respectively (Breysacher, Azzopardi & Testor 1999; Massey, Olsen & Parker 2001). At low metallicity the reduced WR

population and the relative dominance of WN subtypes most likely result from the metallicity dependence of winds from their evolutionary precursors (Mokiem et al. 2007). Consequently, only the most massive single stars reach the WR phase in metal-poor environments. Single stars reaching the WC phase at high metallicity may end their lives as a RSG or WN stars in a lower metallicity environment. As such, one might suspect that most WR stars at low metallicity are formed via binary evolution. However, Foellmi, Moffat & Guerrero (2003a) suggest a similar WR binary fraction for the SMC and Milky Way.

Not all WR subtypes are observed in all environments. Early WN and WC subtypes are preferred in metal-poor galaxies, such as the SMC (Massey et al. 2003), while late WC stars are more common at super-Solar metallicities, such as M83 (Hadfield et al. 2005) Line widths of early WC and WO stars are higher than late WC stars, although width alone is not a defining criterion for each spectral type. The correlation between WC subclass and line width is nevertheless strong (Torres, Conti & Massey 1986). The subtype distributions of WR stars in the Solar Neighbourhood, LMC, and SMC are presented in Figure 3. We shall address this aspect in Sect 4.4.

2.3.3 WR GALAXIES Individual WR stars may, in general, be resolved in Local Group galaxies from ground-based observations, whilst the likelihood of contamination by nearby sources increases at larger distances. For example, a typical slit width of $1''$ at the 2 Mpc distance of NGC 300 corresponds to a spatial scale of $\sim$10 pc. Relatively isolated WR stars have been identified, albeit in the minority (recall Figure 2). This is even more problematic for more distant galaxies such as M 83 where the great majority of WR stars are observed in clusters or associations (Hadfield et al. 2005). So-called 'WR galaxies' are typically starburst

regions exhibiting spectral features from tens, hundreds, or even thousands of WR stars (Schaerer, Contini & Pindao 1999).

Average Milky Way/LMC WN or WC line fluxes (Schaerer & Vacca 1998) are typically used to calculate stellar populations in WR galaxies. These should be valid provided that the line fluxes of WR templates do not vary with environment. However, it is well known that SMC WN stars possess weak emission lines (Conti, Garmany & Massey 1989). In spite of small statistics and a large scatter, the mean He II λ4686 line luminosity of WN2–4 stars in the LMC is $10^{35.9}$ erg s^{-1}, a factor of five times higher than the mean of equivalent stars in the SMC (Crowther & Hadfield 2006). The signature of WN stars is most readily seen in star forming galaxies at He II λ1640, where the dilution from other stellar types is at its weakest (e.g. Hadfield & Crowther 2006). The strongest UV, optical, and near-IR lines indicate flux ratios of I(He II 1640)/I(He II 4686)$\sim$10 and I(He II 4686)/I(He II 1.012μm)$\sim$6 for WN stars spanning SMC to Milky Way metallicities.

Similar comparisons for WC stars are hindered because the only carbon-sequence WR stars at the low metallicity of the SMC and IC 1613 are WO stars. Their emission line fluxes are systematically weaker than WC stars in the LMC and Milky Way (Kingsburgh et al. 1995; Kingsburgh & Barlow 1995; Schaerer & Vacca 1998). The mean C IV $\lambda\lambda$5801-2 line luminosity of WC4 stars in the LMC is $10^{36.5}$ erg s^{-1} (Crowther & Hadfield 2006). Again, detection of WC stars is favoured via ultraviolet spectroscopy of C IV λ1550. For WC stars, the strongest UV, optical, and near-IR lines possess flux ratios of I(C IV 1548-51)/I(C IV 5801-12)$\sim$6 and I(C IV 5801-12)/I(C IV 2.08μm)$\sim$15.

2.4 Binary statistics and masses

The observed binary fraction amongst Milky Way WR stars is 40% (van der Hucht 2001), either from spectroscopic or indirect techniques. Within the low metallicity Magellanic Clouds, close binary evolution would be anticipated to play a greater role because of the diminished role of O star mass-loss in producing single WR stars. However, where detailed studies have been carried out (Bartzakos, Moffat & Niemela 2001; Foellmi, Moffat & Guerrero 2003ab), a similar binary fraction to the Milky Way has been obtained (recall Figure 3), so metallicity-independent LBV eruptions may play a dominant role.

The most robust method of measuring stellar masses is from Kepler's third law of motion, particularly for eclipsing double-lined (SB2) systems, from which the inclination may be derived. Orbital inclinations may also be derived from linear polarization studies (e.g. St-Louis et al. 1993) or atmospheric eclipses (Lamontagne et al. 1996). Masses for Galactic WR stars are included in the van der Hucht (2001) compilation, a subset of which are presented in Figure 4 together with some more recent results. WC masses span a narrow range of 9–16$M_{\odot}$, whilst WN stars span a very wide range of ∼10–83$M_{\odot}$, and in some cases exceed their OB companion, i.e. $q = M_{\rm WR}/M_O > 1$ (e.g. WR22: Schweickhardt et al. 1999). WR20a (SMSP2) currently sets the record for the highest orbital-derived mass of any star, with $\sim 83 M_{\odot}$ for each WN6ha component (Rauw et al. 2005). As discussed above, such stars are H-rich, extreme O stars with strong winds rather than classical H-poor WN stars. They are a factor of two lower in mass than the apparent $\sim 150 M_{\odot}$ stellar mass limit (Figer 2005), such that still more extreme cases may await discovery. Spectroscopic measurement of masses via surface gravities using photospheric lines is not possible for WR stars due to

their dense stellar winds.

2.5 Rotation velocities

Rotation is very difficult to measure in WR stars, since photospheric features – used to estimate $v \sin i$ in normal stars – are absent. Velocities of 200–500 $\mathrm{km\,s^{-1}}$ have been inferred for WR138 (Massey 1980) and WR3 (Massey & Conti 1981), although these are not believed to represent rotation velocities, since the former has a late-O binary companion, and the absorption lines of the latter are formed within the stellar wind (Marchenko et al. 2004). Fortunately, certain WR stars do harbour large scale structures, from which a rotation period may be inferred (St-Louis et al. 2007).

Alternatively, if WR stars were rapid rotators, one would expect strong deviations from spherical symmetry due to gravity darkening (Von Zeipel 1924; Owocki, Cranmer & Gayley 1996). Harries, Hillier & Howarth (1998) studied linear spectropolarimetric datasets for 29 Galactic WR stars, from which just four single WN stars plus one WC+O binary revealed a strong line effect, suggesting significant departures from spherical symmetry. They presented radiative transfer calculations which suggest that the observed continuum polarizations for these stars can be matched by models with equator to pole density ratios of 2–3. Of course, the majority of Milky Way WR stars do not show a strong linear polarization line effect (e.g. Kurosawa, Hillier & Schulte-Ladbeck (1999).

2.6 Stellar wind bubbles

Ring nebulae are observed for a subset of WR stars. These are believed to represent material ejected during the RSG or LBV phases that is photo-ionized

by the WR star. The first known examples, NGC 2359 and NGC 6888, display a shell morphology, although many subsequently detected in the Milky Way and Magellanic Clouds exhibit a variety of spatial morphologies (Chu, Treffers & Kwitter 1983; Dopita et al. 1994). Nebulae are predominantly associated with young WR stars i.e. primarily WN subtypes, with typical electron densities of 10^2 cm^{-3} to 10^3 cm^{-3} (Esteban et al. 1993).

Ring nebulae provide information on evolutionary links between WR stars and their precursors (Weaver et al. 1977). Once a massive star has reached the WR phase, its fast wind will sweep up the material ejected during the immediate precursor (LBV or RSG) slow wind. The dynamical evolution of gas around WR stars with such progenitors has been discussed by García-Segura, MacLow & Langer (1996a) and García-Segura, Langer & MacLow (1996b). Esteban et al. (1993) attempted to derive WR properties indirectly from H II regions associated with selected Milky Way stars (see also Crowther et al. 1999). Unfortunately, relatively few H II regions are associated with individual WR stars, and for the majority of these, the nebular parameters are insufficiently well constrained to distinguish between different stellar atmosphere models.

3 Physical Parameters

3.1 Radiative Transfer

Our interpretation of hot, luminous stars via radiative transfer codes is hindered with respect to normal stars by several effects. First, the routine assumption of LTE breaks down for high-temperature stars. In non-LTE, the determination of populations uses rates which are functions of the radiation field, itself a function of the populations. Consequently, it is necessary to solve for the radiation field

and populations iteratively. Second, the problem of accounting for the effect of millions of spectral lines upon the emergent atmospheric structure and emergent spectrum – known as line blanketing – remains challenging for stars in which spherical, rather than plane-parallel, geometry must be assumed due to stellar winds, since the scale height of their atmospheres is not negligible with respect to their stellar radii. The combination of non-LTE, line blanketing (and availability of atomic data thereof), and spherical geometry has prevented the routine analysis of such stars until recently.

Radiative transfer is either solved in the co-moving frame, as applied by CMFGEN (Hillier & Miller 1998) and PoWR (Gräfener, Koesterke & Hamann 2002) or via the Sobolev approximation, as used by ISA-wind (de Koter, Schmutz & Lamers 1993). The incorporation of line blanketing necessitates one of several approximations. Either a 'super-level' approach is followed, in which spectral lines of a given ion are grouped together in the solution of the rate equations (Anderson 1989), or alternatively, a Monte Carlo approach is followed, which uses approximate level populations (Abbott & Lucy 1985).

3.2 Stellar Temperatures and Radii

Stellar temperatures for WR stars are difficult to characterize, because their geometric extension is comparable with their stellar radii. Atmospheric models for WR stars are typically parameterized by the radius of the inner boundary R_* at high Rosseland optical depth $\tau_{\rm Ross}(\sim 10)$. However, only the optically thin part of the atmosphere is seen by the observer. The measurement of R_* depends upon the assumption that the same velocity law holds for the visible (optically thin) and the invisible (optically thick) part of the atmosphere.

The optical continuum radiation originates from a 'photosphere' where $\tau_{\rm Ross} \sim 2/3$. Typical WN and WC winds have reached a significant fraction of their terminal velocity before they become optically thin in the continuum. $R_{2/3}$, the radius at $\tau_{\rm Ross} = 2/3$ lies at highly supersonic velocities, well beyond the hydrostatic domain. For example, Crowther et al. (2006a) obtain $R_* = 2.9\,R_\odot$ and $R_{2/3} = 7.7\,R_\odot$ for HD 50896 (WN4b), corresponding to $T_* = 85\,$kK and $T_{2/3} = 52\,$kK, respectively. In some weak-lined, early-type WN stars, this is not strictly true since their spherical extinction is modest, in which case $\rm R_* \sim R_{2/3}$ (e.g. HD 9974, Marchenko et al. 2004).

Stellar temperatures of WR stars are derived from lines from adjacent ionization stages of helium or nitrogen for WN stars (Hillier 1987, 1988), or lines of carbon for WC stars (Hillier 1989). High stellar wind densities require the simultaneous determination of mass-loss rate and stellar temperature from non-LTE model atmospheres, since their atmospheres are so highly stratified. Metals such as C, N and O provide efficient coolants, such that the outer wind electron temperature is typically 8 kK to 12 kK (Hillier 1989). Figure 5 compares R_*, $R_{2/3}$, and the principal optical wind line-forming region ($\log n_e = 10^{11}$ to 10^{12} cm^{-3}) for HD 66811 (ζ Pup, O4 I(n)f), HD 96548 (WR40, WN8) and HD 164270 (WR103, WC9) on the same physical scale. Some high-ionization spectral lines (e.g. N V and C IV lines in WN8 and WC9 stars, respectively) are formed at higher densities of $n_e \geq 10^{12}$ cm^{-3} in the WR winds.

Derived stellar temperatures depend sensitively upon the detailed inclusion of line-blanketing by iron peak elements. Inferred bolometric corrections and stellar luminosities also depend upon detailed metal line-blanketing (Schmutz 1997; Hillier & Miller 1999). Until recently, the number of stars studied with

non-LTE, clumped, metal line-blanketed models has been embarrassingly small, due to the need for detailed, tailored analysis of individual stars using a large number of free parameters. Hamann, Gräfener & Liermann (2006) have applied their grid of line-blanketed WR models to the analysis of most Galactic WN stars, for the most part resolving previous discrepancies between alternate line diagnostics, which were first identified by Crowther et al. (1995b). To date, only a limited number of WC stars in the Milky Way and Magellanic Clouds have been studied in detail (e.g. Dessart et al. 2000; Crowther et al. 2002; Barniske, Hamann & Gräfener 2007). Results for Galactic and LMC WR stars are presented in Table 2. These range from 30 kK amongst WN10 subtypes to 40 kK at WN8 and approach 100 kK for early-type WN stars. Spectroscopic temperatures are rather higher for WC stars, i.e. 50 kK for WC9 stars, increasing to 70 kK at WC8 and $\geq$100 kK for early WC and WO stars

Stellar structure models predict radii $R_{\rm evol}$ that are significantly smaller than those derived from atmospheric models. For example, $R_* = 2.7\,R_\odot$ for HD 191765 (WR134, WN6b) in Table 2, versus $R_{\rm evol} = 0.8\,R_\odot$ which follows from hydrostatic evolutionary models, namely

$$\log \frac{R_{\rm evol}}{R_\odot} = -1.845 + 0.338 \log \frac{L}{L_\odot} \qquad (1)$$

for hydrogen-free WR stars (Schaerer & Maeder 1992). Theoretical corrections to such radii are frequently applied, although these are based upon fairly arbitrary assumptions which relate particularly to the velocity law. Consequently, a direct comparison between temperatures of most WR stars from evolutionary calculations and empirical atmospheric models is not straightforward, except that one requires $R_{2/3} > R_{\rm evol}$, with the difference attributed to the extension of the supersonic region. Petrovic, Pols & Langer (2006) established that the hydrostatic

cores of metal-rich WR stars above $\sim 15\ M_\odot$ exceed $R_{\rm evol}$ in Eqn 1 by significant factors if mass-loss is neglected, due to their proximity to the Eddington limit, $\Gamma_e = 1$. Here, the Eddington parameter, Γ_e, is the ratio of radiative acceleration due to Thompson (electron) scattering to surface gravity and may be written as

$$\Gamma_e = 10^{-4.5} q_e \frac{L/L_\odot}{M/M_\odot} \quad (2)$$

where the number of free electrons per atomic mass unit is q_e. In reality, high empirical WR mass-loss rates imply that inflated radii are not expected, such that the discrepancy in hydrostatic radii between stellar structure and atmospheric models has not yet been resolved.

3.3 Stellar Luminosities

Absolute visual magnitudes of WR stars are obtained primarily from calibrations obtained from cluster or association membership (van der Hucht 2001). Inferred bolometric corrections range from $M_{\rm bol} - M_v = $ –2.7 mag amongst very late WN stars (Crowther & Smith 1997) to approximately –6 mag for weak-lined, early-type WN stars and WO stars (Crowther et al. 1995b; Crowther et al. 2000). Stellar luminosities of Milky Way WN stars range from 200,000 $L_\odot$ in early-type stars to 500,000 $L_\odot$ in late-type stars. Hydrogen-burning O stars with strong stellar winds, spectroscopically identified as WNha stars, have luminosities in excess of $10^6\ L_\odot$. For Milky Way WC stars, inferred stellar luminosities are $\sim$150,000 $L_\odot$, increasing by a factor of two for LMC WC stars (Table 2).

Systematically higher spectroscopic luminosities have recently been determined by Hamann, Gräfener & Liermann (2006) for Galactic WN stars, since they adopt uniformly high $M_v = -7.2$ mag for all non-cluster member WN6–9h stars. Absolute magnitudes for normal late-type WN stars are subject to large uncertainties

since such stars positively shy away from clusters. As a consequence, their results suggest a bi-modal distribution around $300,000\ L_{\odot}$ for early WN stars, and 1–2$\times 10^6\ L_{\odot}$ for all late WN stars.

From stellar structure theory, there is a mass-luminosity relation for H-free WR stars which is described by

$$\log \frac{L}{L_{\odot}} = 3.032 + 2.695 \log \frac{M}{M_{\odot}} - 0.461 \left(\log \frac{M}{M_{\odot}} \right)^2 . \qquad (3)$$

This expression is effectively independent of the chemical composition since the continuum opacity is purely electron scattering (Schaerer & Maeder 1992). Spectroscopic luminosities need to be corrected for the luminosity that powers the stellar wind, $\frac{1}{2}\dot{M}v_{\infty}^2$, in order to determine the underlying nuclear luminosity, $L_{\rm nuc}$. In most cases, the recent reduction in estimates of mass-loss rates due to wind clumping (see Sect. 4.3), plus the increase in derived luminosities due to metal line-blanketing indicate a fairly modest corrective factor. From Table 2, one expects typical masses of 10–15 $M_{\odot}$ for hydrogen-free WR stars, which agree fairly well with binary mass estimates (recall Fig. 4). Indeed, spectroscopically derived WR masses obtained using this relationship agree well with binary derived masses (e.g. γ Vel: De Marco et al. 2000).

3.4 Ionizing fluxes

Lyman continuum ionizing fluxes, N(LyC), are typical of mid-O stars in general (Table 2). As such, the low number of WR stars with respect to O stars would suggest that Wolf-Rayet stars play only a minor role in the Lyman continuum ionization budget of young star-forming regions. H-rich late-type WN stars provide a notable exception, since their ionizing output compares closely to O2 stars (Walborn et al. 2004). Crowther & Dessart (1998) showed that the WN6ha stars

in NGC 3603 provided ∼20% of the Lyman continuum ionizing photons, based upon calibrations of non-blanketed models for O and WR stars.

Since WR stars represent an extension of O stars to higher temperatures, significant He I continuum photons are emitted, plus strong He II continua for a few high-temperature, low-density cases. The primary effect of metal-line blanketing is to redistribute extreme UV flux to longer wavelengths, reducing the ionization balance in the wind, such that higher temperatures and luminosities are required to match the observed WR emission line profile diagnostics relative to unblanketed models. Recent revisions to estimated temperatures and luminosities of O stars (as measured from photospheric lines) have acted in the reverse sense, relative to previous plane-parallel unblanketed model analysis, due to backwarming effects, as shown in a number of recent papers (e.g. Martins, Schaerer & Hillier 2002; Repolust, Puls & Herrero 2004). Common techniques are generally now employed for O and WR studies, such that a factor of two increase in N(LyC) for WR stars – plus the reverse for O stars – suggests that in such cases WR stars might provide close to half of the total ionizing photons in the youngest starbursts, such as NGC 3603.

The strength of WR winds affects the hardness of their ionizing radiation. Atmospheric models for WR stars with dense winds produce relatively soft ionizing flux distributions, in which extreme UV photons are redistributed to longer wavelength by the opaque stellar wind (Schmutz, Leitherer & Gruenwald 1992). In contrast, for the low wind-density case, a hard ionizing flux distribution is predicted, in which extreme UV photons pass through the relatively transparent wind unimpeded. Consequently, the shape of the ionizing flux distribution of WR stars depends on both the wind density and the stellar temperature.

We shall show in Section 4 that low-metallicity WR stars possess weaker winds. In Figure 6, we compare the predicted Lyman continuum ionizing flux distribution from four 100 kK WN models, in which only the low metallicity, low mass-loss rate models predicts a prodigious number of photons below the He^+ edge at 228Å. Consequently, one expects evidence of hard ionizing radiation from WR stars (e.g. nebular He II λ4686) solely at low metallicities. This is generally borne out by observations of H II regions associated with WR stars (Garnett et al. 1991). Previous studies of metal-rich regions have claimed a low limit to the stellar mass function from indirect H II region studies at high metallicity in which WR stars were spectroscopically detected. Gonzalez Delgado et al. (2002) were able to reconcile a high stellar mass limit from UV spectral synthesis techniques with a soft ionizing spectrum for the metal-rich WR galaxy NGC 3049 by applying the Smith, Norris & Crowther (2002) line blanketed grid of WR models at high metallicity.

3.5 Elemental abundances

For WR stars, it has long been suspected that abundances represented the products of core nucleosynthesis, although it has taken the development of non-LTE model atmospheres for these to have been empirically supported.

3.5.1 WN AND WN/C STARS Balmer-Pickering decrement studies by Conti, Leep & Perry (1983) concluded that hydrogen was severely depleted in WR stars. A clear subtype effect regarding the hydrogen content of Galactic WN stars is observed, with late-type WN stars generally showing some hydrogen (typically $X_H \sim 15\pm10\%$), and early-type WN stars being hydrogen-free, although exceptions do exist. This trend breaks down within the lower metallicity environment

of the Magellanic Clouds, notably the SMC (Foellmi et al 2003a). Milky Way late-type WN stars with weak emission lines – denoted as 'ha' due to intrinsic absorption lines plus the presence of hydrogen – are universally H-rich with X_H ∼50% (Crowther et al. 1995a; Crowther & Dessart 1998).

Non-LTE analyses confirm that WN abundance patterns are consistent with material processed by the CNO cycle in which these elements are used as catalysts, i.e.

$$^{12}C(p,\gamma)^{13}N(e^-,\nu_e)^{13}C(p,\gamma)^{14}N(p,\gamma)^{15}O(e^-,\nu_e)^{15}N(p,\alpha)^{12}C$$

in which X_N ∼1% by mass is observed in Milky Way WN stars. Carbon is highly depleted, with typically $X_C \sim 0.05\%$. Oxygen suffers from fewer readily accessible line diagnostics, but probably exhibits a similarly low mass fraction as carbon (e.g. Crowther, Smith & Hillier 1995b; Herald, Hillier & Schulte-Ladbeck 2001). Non-LTE analysis of transition WN/C stars reveals elemental abundances (e.g. $X_C \sim 5\%$, $X_N \sim 1\%$ by mass) that are in good agreement with the hypothesis that these stars are in a brief transition stage between WN and WC (Langer 1991; Crowther, Smith & Willis 1995c).

3.5.2 WC AND WO STARS Neither hydrogen nor nitrogen are detected in the spectra of WC stars. Recombination line studies using theoretical coefficients for different transitions are most readily applicable to WC stars, since they show a large number of lines in their optical spectra. Atomic data are most reliable for hydrogenic ions, such as C IV and O VI, so early-type WC and WO stars can be studied most readily. Smith & Hummer (1988) suggested a trend of increasing C/He from late to early WC stars, with C/He=0.04–0.7 by number ($10\% \leq X_C \leq$

60%), revealing the products of core He burning

$$^4He(2\alpha,\gamma)^{12}C \qquad \text{and} \qquad ^{12}C(\alpha,\gamma)^{16}O$$

although significant uncertainties remain in the rate of the latter nuclear reaction. These reactions compete during helium burning to determine the ratio of carbon to oxygen at the onset of carbon burning.

In reality, optical depth effects come into play, so detailed abundance determinations for all subtypes require non-LTE model atmosphere analyses. Koesterke & Hamann (1995) indicated refined values of C/He=0.1–0.5 by number (20% $\leq X_C \leq$ 55%), with no WC subtype dependence, such that spectral types are not dictated by carbon abundance, contrary to suggestions by Smith & Maeder (1991). Indeed, LMC WC4 stars possess similar surface abundances to Milky Way WC stars (Crowther et al. 2002), for which the He II λ5412 and C IV λ5471 optical lines represent the primary diagnostics (Hillier 1989). These recombination lines are formed at high densities of 10^{11} to 10^{12} cm^{-3} at radii of 3–30 R_* (recall Figure 5). Oxygen diagnostics in WC stars lie in the near-UV, such that derived oxygen abundances are rather unreliable unless space-based spectroscopy is available. Where they have been derived, one finds $X_O \sim$ 5–10% for WC stars (e.g. Crowther et al. 2002).

Core He burning in massive stars also has the effect of transforming ^{14}N (produced in the CNO cycle) to neon and magnesium via

$$^{14}N(\alpha,\gamma)^{18}F(e^-,\nu_e)^{18}O(\alpha,\gamma)^{22}Ne(\alpha,n)^{25}Mg$$

and serves as the main neutron source for the s-process in massive stars. Neon lines are extremely weak in the UV/optical spectrum of WC stars (Crowther et al. 2002), but ground-state fine-structure lines at [Ne II] 12.8μm and [Ne III]

15.5μm may be observed via mid-IR spectroscopy, as illustrated for γ Vel in van der Hucht et al. (1996). Fine-structure wind lines are formed at hundreds of stellar radii since their critical densities are of order 10^5 cm^{-3}. Barlow, Roche & Aitken (1988) came to the conclusion that neon was not greatly enhanced in γ Vel with respect to the Solar case ($\sim$0.1% by mass primarily in the form of ^{20}Ne) in γ Vel from their analysis of fine-structure lines. This was a surprising result, since the above reaction is expected to produce $\sim$2% by mass of ^{22}Ne at Solar metallicity.

Once the clumped nature of WR winds is taken into consideration, neon is found to be enhanced in γ Vel and other WC stars (e.g. Dessart et al. 2000). The inferred neon mass fraction is $\sim$1% (see also Crowther, Morris & Smith 2006a). Meynet & Maeder (2003) note that the ^{22}Ne enrichment depends upon nuclear reaction rates rather than stellar models, so the remaining disagreement may suggest a problem with the relevant reaction rates. More likely, a lower metal content is inferred from the neon abundance than Solar metallicity evolutionary models (Z=0.020). Indeed, if the Solar oxygen abundance from Apslund et al. (2004) is taken into account, a revised metal content of Z=0.012 for the Sun is impled. Allowance for depletion of heavy elements due to diffusion in the 4.5 Gyr old Sun suggests a Solar neighbourhood metallicity of Z=0.014 (Meynet, private communication). It is likely that allowance for a reduced CNO content would bring predicted and measured Ne^{22} abundances into better agreement.

WO stars are extremely C- and O-rich, as deduced from recombination analyses (Kingsburgh, Barlow & Storey 1995), and supported by non-LTE models (Crowther et al. 2000). Further nucleosynthesis reactions produce alpha ele-

ments via

$$^{16}O(\alpha,\gamma)^{20}Ne(\alpha,\gamma)^{24}Mg(\alpha,\gamma)^{28}Si(\alpha,\gamma)^{32}S$$

producing a core which is initially dominated by ^{16}O and ^{20}Ne. *Spitzer* studies are in progress to determine neon abundances in WO stars, in order to assess whether these stars show evidence of α–capture of oxygen (in which case enhanced ^{20}Ne would again dominate over ^{22}Ne).

4 Wind Properties

The existence of winds in early-type stars has been established since the 1960's, when the first rocket UV observations (e.g. Morton 1967) revealed the characteristic P Cygni signatures of mass-loss. Electron (Thompson) scattering dominates the continuum opacity in O and WR stars, whilst the basic mechanism by which their winds are driven is the transfer of photon momentum to the stellar atmosphere through the absorption by spectral lines. The combination of a plethora of spectral lines within the same spectral region as the photospheric radiation allows for efficient driving of winds by radiation pressure (Milne 1926). Wind velocities can be directly measured, whilst wind density estimates rely on varying complexity of theoretical interpretation. A theoretical framework for mass-loss in normal hot, luminous stars was developed by Castor, Abbott & Klein (1975), known as CAK theory, via line-driven radiation pressure.

4.1 Wind velocities

The wavelength of the blue edge of saturated P Cygni absorption profiles provides a measure of the asymptotic wind velocity. From these wavelengths, accurate wind velocities of WR stars can readily be obtained (Prinja, Barlow & Howarth

1990; Willis et al. 2004). Alternatively, optical and near-IR He I P Cygni profiles or mid-IR fine-structure metal lines may be used to derive reliable wind velocities (Howarth & Schmutz 1992; Eenens & Williams 1994; Dessart et al. 2000).

In principle, optical recombination lines of He II and C III-IV may also be used to estimate wind velocities, since these are formed close to the asymptotic flow velocity. However, velocities obtained from spectral line modelling are preferable. For WR stars exhibiting weak winds – whose lines are formed interior to the asymptotic flow velocity – only lower velocity limits may be obtained. Nevertheless, observational evidence suggests lower wind velocities at later subtypes by up to a factor of ten than early subtypes (Table 2). Wind velocities of LMC WN stars compare closely with Milky Way counterparts. Unfortunately, UV spectroscopy of SMC WN stars is scarce, such that one has to rely on optical emission lines for wind velocity estimates, which provide only lower limits to terminal wind velocities.

The current record holder amongst non-degenerate stars for the fastest stellar wind is the Galactic WO star WR93b. For it, a wind velocity of 6000 $\mathrm{km\,s^{-1}}$ has been obtained from optical recombination lines (Drew et al. 2004). Individual WO stars have now also been identified in a number of external galaxies. One observes a reduction in line width (and so wind velocity) for stars of progressively lower metallicity, by a factor of up to two between the Milky Way and IC 1613 (Crowther & Hadfield 2006). Although numbers are small, this downward trend in wind velocity with decreasing metallicity is believed to occur for other O and WR spectral types (e.g. Kudritzki & Puls 2000; Crowther 2000).

4.2 Mass-loss rates

The mass-loss rate relates to the velocity field $v(r)$ and density $\rho(r)$ via the equation of continuity

$$\dot{M} = 4\pi r^2 \rho(r) v(r), \tag{4}$$

for a spherical, stationary wind. WR winds may be observed at IR-mm-radio wavelengths via the free-free (Bremsstrahlung) continuum excess caused by the stellar wind or via UV, optical or near-IR emission lines.

Mass-loss rates (e.g. Leitherer, Chapman & Koribalski 1997) follow from radio continuum observations using relatively simple analytical relations, under the assumption of homogeneity and spherical symmetry. The emergent radio flux S_ν depends on the distance to the star d, mass-loss rate and terminal velocity as follows

$$S_\nu \propto \left(\frac{\dot{M}}{v_\infty}\right)^{4/3} \frac{\nu^\alpha}{d^2} \tag{5}$$

(Wright & Barlow 1975), where $\alpha \sim 0.6$ in the constant-velocity regime. Accurate determinations of WR mass-loss rates depend upon composition, ionization balance and electron temperature at physical radii of $\sim 100 - 1000 R_*$. Wind collisions in an interacting binary system will cause additional non-thermal (synchrotron) radio emission (Sect. 5.2), so care needs to be taken against overestimating mass-loss rates in this way.

Optical spectral lines observed in WR stars can be considered as recombination lines, although line formation is rather more complex in reality (Hillier 1988, 1989). Since recombination involves the combination of ion and electron density, the strength of wind lines scales with the square of the density. This explains why only a factor of $\sim$10 increase in wind density with respect to the photospheric absorption line spectrum from O supergiants produces an emission line Wolf-

Rayet spectrum. Recall the comparison of ζ Pup (O4 I(n)f) to HD 96548 (WR40, WN8) in Figure 5.

4.3 Clumping

There is overwhelming evidence in favour of highly clumped winds for WR and O stars. Line profiles show propagating small-scale structures or 'blobs', which are turbulent in nature (e.g. Moffat et al. 1988; Lépine et al. 2000). For optically thin lines, these wind structures have been investigated using radiation hydrodynamical simulations by Dessart & Owocki (2005).

Alternatively, individual spectral lines, formed at $\sim 10R_*$, can be used to estimate volume filling factors f in WR winds (Hillier 1991). This technique permits an estimate of wind clumping factors from a comparison between line electron scattering wings (which scale linearly with density) and recombination lines (density-squared). This technique suffers from an approximate radial density dependence and is imprecise due to severe line blending, especially in WC stars. Nevertheless, fits to UV, optical and IR line profiles suggest $f \sim 0.05-0.25$. As a consequence, global WR mass-loss rates are reduced by a factor of $\sim 2-4$ relative to homogeneous models ($\mathrm{dM/dt} \propto f^{-1/2}$). Representative values are included in Table 2. Spectroscopically derived mass-loss rates of Milky Way WN stars span a wide range of $10^{-5.6}$ to $10^{-4.4} M_\odot$ yr^{-1}. In contrast, Galactic WC stars cover a much narrower range in mass-loss rate, from $10^{-5.0}$ to $10^{-4.4} M_\odot$ yr^{-1}.

Independent methods support clumping-corrected WR mass-loss rates. Binary systems permit use of the variation of linear polarization with orbital phase. The modulation of linear polarization originates from Thomson scattering of free electrons due to the relative motion of the companion with respect to the WR

star. This technique has been applied to several WR binaries including V444 Cyg (HD 193576=WR139, WN5+O) by St-Louis et al. (1993) and has been developed further by Kurosawa, Hillier & Pittard (2002) using a Monte Carlo approach. For the case of V444 Cyg, polarization results suggest a clumping factor of $f \sim 0.06$.

The most likely physical explanation for the structure in WR and O star winds arises from theoretical evidence supporting an instability in radiatively-driven winds (Lucy & Solomon 1971; Owocki, Castor & Rybicki 1988). There is a strong potential in line scattering to drive wind material with accelerations that greatly exceed the mean outward acceleration. Simulations demonstrate that this instability may lead naturally to structure. Such a flow is dominated by multiple shock compressions, producing relatively soft X-rays. Hard X-ray fluxes from early-type stars are believed to be restricted to colliding wind binary systems (e.g. γ Vel: Schild et al. 2004), for which $10^{-7} \leq L_X/L_{\rm bol} \leq 10^{-6}$.

4.4 Metallicity dependent winds?

We shall now consider empirical evidence in favour of metallicity-dependent WR winds. Nugis, Crowther & Willis (1998) estimated mass-loss rates for Galactic WR stars from archival radio observations, allowing for clumped winds. Nugis & Lamers (2000) provided empirical mass-loss scaling relations by adopting physical parameters derived from spectroscopic analysis and/or evolutionary predictions. For a combined sample of WN and WC stars, Nugis & Lamers (2000) obtained

$$\log \dot{M}/(M_{\odot}{\rm yr}^{-1}) = -11.00 + 1.29 \log L/L_{\odot} + 1.74 \log Y + 0.47 \log Z \quad (6)$$

where Y and Z are the mass fractions of helium and metals, respectively.

4.4.1 WN WINDS Smith & Willis (1983) compared the properties of WN stars in the LMC and Milky Way, concluding there was no significant differ-

ences between the wind properties of the two samples. These conclusions were supported by Hamann & Koesterke (2000) from detailed non-LTE modelling, although a large scatter in mass-loss rates within each parent galaxy was revealed. Either there is no metallicity dependence, or any differences are too subtle to be identified from the narrow metallicity range spanned by the Milky Way and LMC. Within the Milky Way, most late-type stars contain hydrogen and most early-type stars do not. In contrast, early-type stars dominate WN populations in the Magellanic Clouds (recall Figure 3), and often contain atmospheric hydrogen (Smith, Shara & Moffat 1996; Foellmi, Moffat & Guerrero 2003ab).

Figure 7 compares the mass-loss rates of cluster or association member WN stars in the Milky Way with Magellanic Cloud counterparts. Mass-loss estimates are obtained from their near-IR helium lines (Crowther 2007, following Howarth & Schmutz 1992). The substantial scatter in mass-loss rates is in line with the heterogeneity of line strengths within WN subtypes. Stronger winds are measured for WN stars without surface hydrogen, in agreement with Eqn 6) and recent results of Hamann, Gräfener & Liermann (2006). From the Figure, measured mass-loss rates of hydrogen-rich early-type WN stars in the SMC (1/5 $Z_{\odot}$) are 0.4 dex weaker than equivalent stars in the Milky Way and LMC (1/2 to 1 $Z_{\odot}$). This suggests a metallicity dependence of dM/dt $\propto Z^m$ for WN stars, with $m \sim 0.8 \pm 0.2$. The exponent is comparable to that measured from Hα observations of Milky Way, LMC and SMC O-type stars (Mokiem et al. 2007).

There are two atmospheric factors which contribute to the observed trend towards earlier WN subtypes at lower metallicities;

1. CNO compromises ∼1.1% by mass of the Solar photosphere (Asplund et al. 2004) versus 0.48% in the LMC and 0.24% in the SMC (Russell & Dopita

1990). Since WN stars typically exhibit CNO equilibrium abundances, there is a maximum nitrogen content available in a given environment. For otherwise identical physical parameters, Crowther (2000) demonstrated that a reduced nitrogen content at lower metallicity favours an earlier subtype. This is regardless of metallicity dependent mass-loss rates, and results from the abundance sensitivity of nitrogen classification lines.

2. Additionally, a metallicity dependence of WN winds would enhance the trend to earlier spectral subtypes. Dense WN winds at high metallicities lead to efficient recombination from high ionization stages (e.g. N^{5+}) to lower ions (e.g. N^{3+}) within the optical line formation regions. This would not occur so effectively for low density winds, enhancing the trend towards early-type WN stars in metal-poor environments.

Consequently, both effects favour predominantly late subtypes at high metallicity, and early subtypes at low metallicity, which is indeed generally observed (Fig. 3).

4.4.2 WC WINDS It is well established that WC stars in the inner Milky Way, and indeed all metal-rich environments, possess later spectral types than those in the outer Galaxy, LMC and other metal-poor environments (Figure 3; Hadfield et al. 2007). This observational trend led Smith & Maeder (1991) to suggest that early-type WC stars are richer in carbon than late-type WC stars, on the basis of tentative results from recombination line analyses. In this scenario, typical Milky Way WC5–9 stars exhibit reduced carbon abundances than WC4 counterparts in the LMC. However, quantitative analysis of WC subtypes allowing for radiative transfer effects do not support a subtype dependence of elemental abundances in WC stars (Koesterke & Hamann 1995), as discussed in Sect 3.5.

If differences of carbon content are not responsible for the observed WC subtype distribution in galaxies, what is its origin? Let us consider the WC classification lines – C III λ5696 and C IV $\lambda\lambda$5801-12 – in greater detail. Specifically the upper level of λ5696 has an alternative decay via λ574, with a branching ratio of 147:1 (Hillier 1989). Consequently λ5696 only becomes strong when λ574 is optically thick, i.e. if the stellar temperature is low *or* the wind density is sufficiently high. From non-LTE models it has been established that the temperatures of Galactic WC5–7 stars and LMC WC4 stars are similar, such that the observed subtype distribution argues that the wind densities of Galactic WC stars must be higher than the LMC stars.

Figure 7 also compares clumping corrected mass-loss rates of WC stars in the Milky Way and LMC, as derived from optical studies. The Galactic sample agree well with Eqn 6 from Nugis & Lamers (2000). Crowther et al. (2002) obtain a similar mass-loss dependence for WC4 stars in the LMC, albeit offset by –0.25 dex. The comparison between derived LMC and Solar neighbourhood WC wind properties suggests a dependence of $\mathrm{dM/dt} \propto Z^m$ with $m \sim 0.6 \pm 0.2$. Crowther et al. (2002) argued that the WC subtype distributions in the LMC and Milky Way resulted from this metallicity dependence. C III λ5696 emission is very sensitive to mass-loss rate, so weak winds for LMC WC stars would produce negligible C III λ5696 emission (WC4 subtypes) and strong winds interior to the Solar circle would produce strong C III λ5696 emission (WC8-9 subtypes), in agreement with the observed subtype distributions.

4.5 Line driving in WR winds

Historically, it has not been clear whether radiation pressure alone is sufficient to drive the high mass-loss rates of WR stars. Let us briefly review the standard Castor, Abbott & Klein (1975, hereafter CAK) theory behind radiatively driven winds before addressing the question of line driving for WR stars. Pulsations have also been proposed for WR stars, as witnessed in intensive monitoring for the most photometrically variable WN8 star with the *MOST* satellite by Lefévre et al. (2005). Interpretation of such observations however remains ambiguous (Townsend & MacDonald 2006; Dorfi, Gautschy & Saio 2006).

4.5.1 Single scattering limit The combination of plentiful line opacity in the extreme UV, where the photospheric radiation originates, allows for efficient driving of hot star winds by radiation pressure (Milne 1926). In a static atmosphere, the photospheric radiation will only be efficiently absorbed or scattered in the lower layers of the atmosphere, weakening the radiative acceleration, $g_{\rm line}$, in the outer layers. In contrast, atoms within the outer layers of an expanding atmosphere see the photosphere as Doppler-shifted radiation, allowing absorption of undiminished continuum photons in their line transitions (Sobolev 1960).

The force from optically thick lines, which provide the radiative acceleration by absorbing the photon momentum, scale with the velocity gradient. There can be at most $\approx c/v_\infty$ thick lines, implying a so-called single-scattering limit

$$\dot{M} v_\infty \leq L/c. \tag{7}$$

Castor, Abbott & Klein (1975) and Abbott (1982) developed a self-consistent

solution of the wind properties, from which one obtains a velocity 'law'

$$v(r) = v_\infty \left(1 - \frac{R_*}{r}\right)^\beta , \tag{8}$$

for which β=0.8 for O-type stars (Pauldrach, Puls & Kudritzki 1986). $g_{\rm line}$ can be written in terms of the Thompson (electron) scattering acceleration, i.e. $g_{\rm line} = g_e X(t)$. The equation of motion can then be expressed as

$$v\frac{dv}{dr} = \frac{GM}{r^2}\left(\Gamma_e(1 + X(t)) - 1\right). \tag{9}$$

It is clear that both Γ_e and $X(t)$ need to be large for a hot star to possess a wind. In the CAK approach, optically thick lines are assumed not to overlap within the wind. In reality, this is rarely true in the extreme UV where spectral lines are very tightly packed and the bulk of the line driving originates. Consequently, another approach is needed for WR stars whose winds exceed the single scattering limit (Lamers & Leitherer 1993), namely the consideration of multiple scattering.

4.5.2 Multiple scattering Historically, the strength of WR winds were considered to be mass dependent, but metallicity-independent (Langer 1989). Observational evidence now favours metallicity-dependent WR winds, with a dependence of dM/dt $\propto Z^m$, with $m \sim 0.8$ for WN stars (Sect. 4.4). It is established that O star winds are driven by radiation pressure, with a metallicity dependence that is similar to WN stars (Mokiem et al. 2007). Consequently, the notion that WR winds are radiatively driven is observationally supported.

Theoretically, Lucy & Abbott (1993) and Springmann (1994) produced Monte Carlo wind models for WR stars in which multiple-scattering was achieved by the presence of multiple ionization stages in the wind. However, a prescribed velocity and ionization structure was adopted in both case studies, plus the inner wind acceleration was not explained.

Schmutz (1997) first tackled the problem of driving WR winds from radiatively-driven winds self-consistently using a combined Monte Carlo and radiative transfer approach. He also introduced a means of photon-loss from the He II Lyα 303Å line via a Bowen resonance-fluorescence mechanism. This effect led to a change in the ionization equilibrium of helium, requiring a higher stellar luminosity. The consideration of wind clumping by Schmutz (1997) did succeed in providing a sufficiently strong outflow in the outer wind. Photon-loss nevertheless failed to initiate the requisite powerful acceleration in the deep atmospheric layers. Subsequent studies have supported the principal behind the photon-loss mechanism for WR stars, although the effect is modest (e.g. De Marco et al. 2000).

The next advance for the inner wind driving was by Nugis & Lamers (2002) whose analytical study suggested that the (hot) iron opacity peak at $10^{5.2}$ K is responsible for the observed WR mass-loss in an optically thick wind (a cooler opacity peak exists at $10^{4.6}$K). Indeed, Gräfener & Hamann (2005) established that highly ionized Fe ions (Fe IX-XVII) provides the necessary opacity for initiating WR winds deep in the atmosphere for WR111 (HD 165763=WR111, WC5). The wind acceleration due to radiation and gas pressure self-consistently matches the mechanical and gravitational acceleration in their hydrodynamical model. Gräfener & Hamann (2005) achieved the observed terminal wind velocity by adopting an extremely low outer wind filling factor of f=0.02. This degree of clumping is unrealistic since predicted line electron scattering wings are too weak with respect to observations. A more physical outer wind solution should be permitted by the inclusion of more complete opacities from other elements such as Ne and Ar. The velocity structure from the Gräfener & Hamann (1995) hydrodynamical model closely matches a typical β=1 velocity law of the form in

Eqn 8 in the inner wind. A slower β=5 law is more appropriate for the outer wind. Indeed, such a hybrid velocity structure was first proposed by Hillier & Miller (1999).

Theoretically, both the hydrodynamical models of Gräfener & Hamann (2005) and recent Monte Carlo wind models for WR stars by Vink & de Koter (2005) argue in favour of radiation pressure through metal lines as responsible for the observed multiple-scattering in WR winds. The critical parameter involving the development of strong outflows is the proximity of WR stars to the Eddington limit, according to Gräfener & Hamann (2007).

Vink & de Koter (2005) performed a multiple-scattering study of WR stars at fixed stellar temperatures and Eddington parameter. A metallicity scaling of dM/dt $\propto Z^m$ with m=0.86 for $10^{-3} \leq Z/Z_{\odot} \leq 1$ was obtained. This exponent is similar to empirical WN and O star results across a more restricted metallicity range. Gräfener & Hamann (2007) predict a decrease in the exponent or late-type WN stars at higher Γ_e, plus reduced wind velocities at lower metallicities. Vink & de Koter (2005) predict that the high metal content of WC stars favour a weaker dependence with metallicity than WN stars. A mass-loss scaling with exponent m=0.66 for $10^{-1} \leq Z/Z_{\odot} \leq 1$ is predicted. This is consistent with the observed WC mass-loss dependence between the LMC and Milky Way. At low metallicity, Vink & de Koter (2005) predict a weak dependence of m=0.35 for $10^{-3} \leq Z/Z_{\odot} \leq 10^{-1}$ providing atmospheric carbon and oxygen abundances are metallicity-independent.

5 Interacting Binaries

5.1 Close binary evolution

The components of a massive binary may evolve independently, as if they were single stars providing their orbital periods are sufficiently large. In contrast, an interacting or close binary system represents the case in which the more massive primary component expands to fill its Roche lobe, causing mass exchange to the secondary. For an initial period of several days, the primary will reach its Roche lobe whilst still on the H-core burning main sequence (Case A) and transfer the majority of its hydrogen-rich envelope to the secondary. For initial periods of a few weeks or years, mass transfer will occur during the hydrogen-shell burning phase (Case B) or He-shell burning (Case C), respectively. Cases B and C are much more common than Case A due to the much larger range of orbital periods sampled. According to Vanbeveren, De Loore & Van Rensbergen (1998) a common envelope will occur instead of Roche lobe overflow if there is an LBV phase.

Close binary evolution will extend the formation of WR stars to lower initial mass, and consequently lower luminosity with respect to single star evolution (e.g. Vanbeveren et al. 1998). The observed lower mass limit to WR formation in the Milky Way is broadly consistent with the single star scenario (Meynet & Maeder 2003). Therefore, either low-mass He stars are not recognised spectroscopically as WR stars, or they may be too heavily diluted by their brighter O star companions for them to be observed.

One natural, albeit rare, consequence of massive close binary evolution involves the evolution of the initial primary to core-collapse, with a neutron star or black

hole remnant, in which the system remains bound as a high mass X-ray binary (HMXB, Wellstein & Langer 1999). The OB secondary may then evolve through to the Wolf-Rayet phase, producing a WR plus neutron star or black hole binary. For many years, searches for such systems proved elusive, until it was discovered that Cyg X–3, a 4.8 hour period X-ray bright system possessed the near-IR spectrum of a He-star (van Kerkwijk et al. 1992). Nevertheless, the nature of Cyg X–3 remains somewhat controversial. WR plus compact companion candidates have also been identified in external galaxies, IC 10 X–1 (Bauer & Brandt 2004) and NGC 300 X-1 (Carpano et al. 2007).

5.2 Colliding winds

The presence of two early-type stars within a binary system naturally leads to a wind-wind interaction region. In general, details of the interaction process are investigated by complex hydrodynamics. Nevertheless, the analytical approach of Stevens, Blondin & Pollock (1992) provides a useful insight into the physics of the colliding winds.

A subset of WR stars display non-thermal (synchrotron) radio emission, in addition to the thermal radio emission produced via free-free emission from their stellar wind. Consequently, a magnetic field must be present in the winds of such stars, with relativistic electrons in the radio emitting region. Shocks associated with a wind collision may act as sites for particle acceleration through the Fermi mechanism (Eichler & Usov 1993). Free electrons would undergo acceleration to relativistic velocities by crossing the shock front between the interacting stellar winds. Indeed, the majority of non-thermal WR radio emitters are known binaries. For example, WR140 (WC7+O) is a highly eccentric system with a 7.9 year

period, in which the radio flux is thermal over the majority of the orbit. Between phases 0.55 and 0.95 (where phase 0 corresponds to periastron passage), the radio flux increases dramatically and displays a non-thermal radio index (Williams et al. 1990).

One may introduce the wind momentum ratio, R

$$R = \frac{\dot{M}_1 v_{\infty,1}}{\dot{M}_2 v_{\infty,2}} \tag{10}$$

where the mass loss rates and wind velocities of components i are given by $\dot{M}_i$ and $v_{\infty,i}$, respectively. In the simplest case of R=1, the intersection between the winds occurs in a plane midway between the two stars. In the more likely situation of $R \neq 1$, the contact discontinuity appears as a cone wrapped around the star with the less momentum in its wind. By way of example, radio emission in the WR147 (WN8 + B0.5) system has been spatially resolved into two components: thermal emission from the WN8 primary wind, plus non-thermal emission located close to the companion (Williams et al. 1997). The location of the non-thermal component is consistent with the ram pressure balance of the two stellar winds, from which a momentum ratio of $R \sim 0.011$ can be obtained.

For early-type stars that have reached their terminal velocities of several thousand $\mathrm{km\,s^{-1}}$, the post-shock plasma temperature is very high ($\geq 10^7$ K). X-rays represent the main observational signature of shock-heated plasma. Significantly harder X-ray fluxes are expected from massive binaries with respect to single stars. Phase-locked X-ray variability is expected due to the change in opacity along the line-of-sight, or varying separation for eccentric binaries (Stevens, Blondin & Pollock 1992). A colliding wind system in which substantial phase-locked variability has been observed with *ROSAT* is γ Vel (WC8+O). The X-ray emission from the shock is absorbed when the opaque wind from the WR star

lies in front of the O star. When the cavity around the O star crosses our line-of-sight, X-ray emission is significantly less absorbed (Willis, Schild & Stevens 1995).

5.3 Dust formation

The principal sources of interstellar dust are cool, high mass-losing stars, such as red giants, asymptotic giant branch stars, plus novae and supernovae. Dust is observed around some massive stars, particularly LBVs with ejecta nebulae, but aside from their giant eruptions, this may be material that has been swept up by the stellar wind. The intense radiation fields of young, massive stars would be expected to prevent dust formation in their local environment. However, Allen, Swings & Harvey (1972) identified excess IR emission in a subset of WC stars, arising from $\sim$1000 K circumstellar dust.

Williams, van der Hucht & Thé (1987) investigated the infrared properties of Galactic WC stars, revealing persistent dust formation in some systems, or episodic formation in other cases. For a single star whose wind is homogeneous and spherically symmetric, carbon is predicted to remain singly or even doubly ionized due to high electron temperatures of $\sim 10^4$K in the region where dust formation is observed to occur. However, the formation of graphite or more likely amorphous carbon grains requires a high density of neutral carbon close to the WC star.

One clue to the origin of dust is provided by WR140 (HD 193793, WC7+O) which forms dust episodically, near periastron passage. At this phase the power in the colliding winds is at its greatest (Williams et al. 1990). Usov (1991) analytically showed that the wind conditions of WR140 at periastron favour a strong

gas compression in the vicinity of the shock surface, providing an outflow of cold gas. It is plausible that high density, low temperature, carbon-rich material associated with the bow-shock in a colliding wind WC binary provides the necessary environment for dust formation.

In contrast to episodic dust formers, persistent WC systems are rarely spectroscopic WC binaries, for which WR104 (Ve 2-45, WC9) is the prototype identified by Allen et al. (1972). Spectroscopic evidence from Crowther (1997) suggested the presence of an OB companion in the WR104 system when the inner WC wind was obscured by a dust cloud, analogous to R Coronae Borealis stars. Conclusive proof of the binary nature of WR104 has been established by Tuthill, Monnier & Danchi (1999) from high spatial resolution near-IR imaging. Dust associated with WR104 forms a spatially confined stream that follows a spiral trajectory (so-called 'pinwheel'), analogous to a garden rotary sprinker. The cocoon stars after which the Quintuplet cluster at the Galactic Centre was named have also been identified as dusty WC pinwheel stars by Tuthill et al. (2006).

Binarity appears to play a key role in the formation of dust in WC stars, providing the necessary high density within the shocked wind interaction region, plus shielding from the hard ionizing photons. The presence of hydrogen from the OB companion may provide the necessary chemical seeding in the otherwise hydrogen-free WC environment. Alas, this possibility does have difficulties, since chemical mixing between the WC and OB winds may not occur in the immediate vicinity of the shock region. Nevertheless, it is likely that all dust forming WC stars are binaries.

6 Evolutionary models and properties at core-collapse

The various inputs to stellar interior evolutionary models originate from either laboratory experiments (e.g. opacities, nuclear reaction rates) or astronomical observations (e.g. mass-loss properties, rotation rates). Indeed, mass-loss (rather than convection) has a dominant effect upon stellar models for the most massive stars.

Here we illustrate one of the potential pitfalls of this approach. According to Koesterke et al. (1991), stellar luminosities of some weak-lined early-type WN stars were unexpectedly low ($\leq 10^5 L_\odot$). In order to reproduce such results, plus the observed N(WR)/N(O) ratio, Meynet et al. (1994) adopted higher stellar mass-loss rates, with respect to previous empirical calibrations. Improvements in non-LTE models have subsequently led to higher derived stellar luminosities (e.g. Hamann, Gräfener & Liermann 2006). Revised WR luminosities removed the primary motivation behind elevated mass-loss rates. Indeed, allowance for wind clumping has now led to the need to reduce mass-loss rates in evolutionary models.

6.1 Rotational mixing

Mass-loss and rotation are intimately linked for the evolution of massive stars. Stellar winds will lead to spin-down for the case of an efficient internal angular momentum transport mechanism. At Solar metallicity, one anticipates rapid spin-down for very massive stars due to their strong stellar winds (Langer 1998). Initial rotational velocities are erased within a few million years. In contrast, initial conditions may remain preserved throughout the main sequence lifetime of O-type stars in metal-poor environments due to their weak stellar winds.

Discrepancies between evolutionary model predictions and a number of observed properties of high mass stars led to the incorporation of rotational mixing into interior models, following the theoretical treatment of Zahn (1992). Rotational mixing reproduces some of the predictions from the high mass-loss evolutionary models of Meynet et al. (1994), for which two approaches have been developed. Meynet & Maeder (1997) describe the transport of angular momentum in the stellar interior through the shear and meridional instabilities. In contrast, momentum is transported radially from the core to the surface in the approach of Heger et al. (2000).

Rotation favours the evolution into the WR phase at earlier stages, increasing the WR lifetime. Lower initial mass stars also enter the WR phase. For an assumed initial rotational velocity of 300 $\mathrm{km\,s^{-1}}$, the minimum initial mass star entering the WR phase is 22 $M_\odot$, versus $37M_\odot$ for non-rotating models at Solar metallicity (Meynet & Maeder 2003). Evolutionary models allowing for rotational mixing do predict a better agreement with the observed ratio of WR to O stars at low metallicity, the existence of intermediate WN/C stars (though see Langer 1991), and the ratio of blue to red supergiants in galaxies.

Regarding the initial rotation velocities of massive stars, evolutionary models adopt fairly high values. Observationally, $v_{\rm rot} \sim 175 \pm 125$ $\mathrm{km\,s^{-1}}$ for young OB stars in the SMC cluster NGC 346 (Mokiem et al. 2006), suggesting somewhat lower initial rotation rates, on average. Nevertheless, lower mass limits to the formation of WR stars are predicted to lie in the range $42M_\odot$ at Z=0.004 (SMC) to $21M_\odot$ at Z=0.04 (M 83) for models allowing for such high initial rotation rates (Meynet & Maeder 2005). Hirschi, Meynet & Maeder (2005) present chemical yields from rotating stellar models at Solar metallicity, revealing increased C and

O yields below $30M_{\odot}$, and higher He yields at higher initial masses.

6.2 Evolutionary model predictions

It is possible to predict the number ratio of WR to O stars for regions of constant star formation from rotating evolutionary models, weighted over the Initial Mass Function (IMF). For an assumed Salpeter IMF slope for massive stars, the ratios predicted are indeed in much better agreement with the observed distribution at Solar metallicity (Meynet & Maeder 2003). Since the O star population is relatively imprecise, the predicted WR subtype distributions are often used instead for comparisons with observations.

From Figure 3, the Solar Neighbourhood WR subtype distribution contains similar numbers of WC and WN stars, with an equal number of early (H-free) and late (H-rich) WN stars. From comparison with evolutionary models, the agreement is reasonable, except for the brevity of the H-deficient WN phase in interior models at Solar metallicity. This aspect has been quantified by Hamann, Gräfener & Liermann (2006). Synthetic WR populations from the Meynet & Maeder (2003) evolutionary tracks predict that only 20% of WN stars should be hydrogen-free, in contrast to over 50% of the observed sample. Non-rotating models provide better statistics, although low luminosity early-type WN stars are absent in such synthetic populations.

Figure 8 shows that the ratio of WC to WN stars is observed to increase with metallicity for nearby galaxies whose WR content has been studied in detail. One notably exception is the low-metallicity Local Group galaxy IC 10 (Massey & Holmes 2002; Crowther et al. 2003). The WR population of IC 10 remains controversial, since high Galactic foreground extinction favours the detection of

WC stars over WN stars. The preferential detection of WC stars arises because the equivalent widths of the strongest optical lines in WC stars are (up to 100 times) larger than those of the strongest optical lines in WN stars (Massey & Johnson 1998).

Two evolutionary model predictions are included in Fig. 8; (a) allowing for rotational mixing but without a WR metallicity scaling (Meynet & Maeder 2005); (b) neglecting rotational mixing, although with a metallicity scaling for WR stars (Eldridge & Vink 2006). The latter models, in which convective overshooting is included, agree better with observations at higher metallicities. It should be emphasised that a significant WR population formed via a close binary channel is required to reproduce the observed WR/O ratio across the full metallicity range in the Eldridge & Vink (2006) models (see also Van Bever & Vanbeveren 2003). A significant binary channel is not required for the Meynet & Maeder (2005) rotating evolutionary models. These resolve many issues with respect to earlier comparisons to observations, although some problems persist.

In very metal-poor environments ($\sim$1/50 $Z_{\odot}$) the WR phase is predicted for only the most massive single stars ($\geq 90 M_{\odot}$) according to non-rotating models of de Mello et al. (1998). Nevertheless, WR stars have been observed in UV and optical spectroscopy of such metal-poor regions within I Zw 18 (Izotov et al. 1997; Brown et al. 2002) and SBS 0335-052E (Papaderos et al. 2006). Only WC stars have been unambiguously identified spectroscopically, yet WN stars would be expected to dominate the WR population of such metal-poor regions. The strength of WN winds are believed to depend more sensitively upon metallicity than the strength of WC winds (Vink & de Koter 2005). Therefore, WN stars may be extremely difficult to directly detect. Hot weak-lined WN stars are predicted

to have hard UV ionizing flux distributions, so they may be indirectly indicated via the presence of strong nebular He II λ4686 emission. Indeed, strong nebular He II λ4686 is observed in I Zw 18, SBS 0335-052E and other very metal-poor star forming galaxies.

Potentially large WR populations are inferred in very metal-deficient galaxies, depending upon the exact WR wind dependence upon metallicity (Crowther & Hadfield 2006). Potentially, single star rotating evolutionary models are unable to reproduce the observed WR distribution in metal-poor galaxies. Close binary evolution might represent the primary formation channel for such metal-poor WR stars, unless LBV eruptions provide the dominant method of removing the H-rich envelope at low metallicity.

6.3 WR stars as SNe and GRB progenitors

The end states of massive stars have been studied from a theoretical perspective by Heger et al. (2003). In particular, WN and WC stars are the likely progenitors of (at least some) Type Ib and Type Ic core-collapse SN, respectively. This arises because, respectively hydrogen and hydrogen/helium are absent in such SNe (Woosley & Bloom 2006). Direct empirical evidence connecting single WR stars to Type Ib/c SN is lacking, for which lower mass interacting binaries represent alternative progenitors. One would need observations of $\geq 10^4$ WR stars in order to firmly establish a connection on a time frame of a few years, since WR lifetimes are a few 10^5 yr (Meynet & Maeder 2005). Hadfield et al. (2005) identified 10^3 WR stars in M83. Narrow-band optical surveys of a dozen other high star-forming spiral galaxies within $\sim$10 Mpc would likely provide the necessary statistics. However, ground-based surveys would be hindered by the

relatively low spatial resolution of 20 pc per arcsec at 5 Mpc.

Nevertheless, the light curves of broad-lined Type Ic supernovae – SN 1998bw, SN 2003dh and SN 2003lw – suggest ejected core masses of order $10M_{\odot}$ (Nakamura et al. 2001; Mazzali et al. 2003; Malesani et al. 2004). These agree rather well with the masses of LMC WC4 stars inferred by Crowther et al. (2002), if we additionally consider several solar masses which remain as a compact (black hole) remnant. Tese supernovae were associated with long GRBs, namely 980425 (Galama et al. 1998), 030329 (Hjorth et al. 2003), and 031203 (Malesani et al. 2004), in support of the 'collapsar' model (MacFadyen & Woosley 1999). Indeed, WR populations have been detected in the host galaxy of GRB 980425, albeit offset from the location of the GRB by several hundred pc (Hammer et al. 2006). Perhaps GRBs are produced by runaway WR stars, ejected from high density star clusters (Cantiello et al. 2007)? Such a scenario would appear to contradict Fruchter et al. (2006), regarding the location of GRBs in their host galaxies.

The challenge faced by both single and binary evolutionary models is for a rotating core at the point of core-collapse (Woosley & Heger 2006). Single star models indicate that stars efficiently spin-down during either: (a) the slowly rotating RSG stage – due to the magnetic dynamo produced by differential rotation between the rotating He-core and non-rotating H-envelope; (b) the mechanical loss of angular momentum from the core during the high mass-loss WR phase. Spectropolarimetry does not favour rapid rotation for Milky Way WC stars, although some WN stars may possess significant rotation rates.

Typical magnetic fields of neutron stars are of order 10^{12} G, so one would expect a field of 10^2 G for their progenitor Wolf-Rayet stars. The first observational limits are now becoming available, namely $\leq$25 G for HD 50896 (WR6, St-Louis

et al. 2007). If WR stars are credible progenitors of 'magnetars', a subset of neutron stars that are highly magnetized ($\sim 10^{15}$ G), the required WR magnetic field would be $\sim 10^3$ G.

Initial rapid rotation of a single massive star may be capable of circumventing an extended envelope via chemically homogeneous evolution (Maeder 1987) if mixing occurs faster than the chemical gradients from nuclear fusion. At sufficiently low metallicity, mechanical mass-loss during the WR phase would be sufficiently weak to prevent loss of significant angular momentum permitting the necessary conditions for a GRB (Yoon & Langer 2005). Alternatively, close binary evolution could cause the progenitor to spin-up due to tidal interactions or the merger of a black hole and He core within a common envelope evolution (Podsiadlowski et al. 2004). Both single and binary scenarios may operate. At present, the single scenario is favoured since long-soft GRBs are predominantly observed in host galaxies which are fainter, more irregular and more metal-deficient than hosts of typical core-collapse supernovae (e.g. Fruchter et al. 2006).

Of course, the ejecta strongly interact with the circumstellar material, probing the immediate vicinity of the GRB itself (van Marle, Langer & García-Segura 2005). This provides information on the progenitor, for which one expects $\rho \propto r^{-2}$ for WR winds (Eqn 4). A metallicity-dependence of WR winds suggests that one would potentially expect rather different environments for the afterglows of long-duration GRBs, depending upon the metallicity of the host galaxy. Indeed, densities of the immediate environment of many GRBs suggest values rather lower than typical Solar metallicity WR winds (Chevalier, Li & Frasson 2004). Fryer, Rockefeller & Young (2006) estimate half of long GRBs apparently occur in uniform environments, favouring a post-common envelope binary merger model.

7 Summary Points

1. The agreement between multi-wavelength spectroscopic observations of WR stars and current non-LTE model atmospheres is impressive. H-rich (core H-burning) WN stars are readily distinguished from classic H-deficient (core He-burning) WN, WC and WO stars. Significant progress has been achieved in interior evolutionary models through the incorporation of rotational mixing. Contemporary (i.e. low) mass-loss rates together with rotational mixing permits many of the observed properties of WR stars to be reproduced, at least those close to Solar metallicity.

2. Empirical evidence and theoretical models both favour metallicity-dependent WR wind, providing a natural explanation to the WC (and WO) subtype distribution in the Milky Way and in external galaxies. A metallicity dependence is partially responsible for the WN subtype dependence, although the reduced nitrogen content in metal-poor galaxies also plays a role. The development of consistent radiatively-driven WR winds represents an important milestone. The predicted metallicity dependence of mass-loss rates from radiatively driven wind models agrees with observational estimates.

3. The apparent convergence of spectroscopic and interior models suggests that we can re-assess the contribution of WR stars to the ionizing, mechanical and chemical enrichment of the ISM in young star forming regions with respect to the previous Annual Review article on this subject (Abbott & Conti 1987). WR stars emit a high number of Lyman continuum photons due to higher inferred stellar luminosities as a result of the inclusion of line blanketing in atmospheric models. Inferred WR mass-loss rates have

decreased due to overwhelming evidence in favour of clumped winds. The chemical enrichment from WR stars is believed to be significant due to an extended WC phase, as a result of rotational mixing within evolutionary models.

8 Future Issues to be Resolved

1. Current non-LTE models rely upon a simplified clumpy wind structure, plus spherical symmetry. Theoretical hydrodynamic predictions for the radial dependence of clumping in WR winds is anticipated to represent a major area of development over the next decade together with two dimensional non-LTE radiative transfer codes.

2. Discrepancies persist between empirical WR populations and predictions from evolutionary models which allow for rotational mixing. Metallicity dependent WR winds may improve consistency, together with the incorporation of magnetic fields. Spatially resolved clusters rich in WR stars, such as Westerlund 1 (if it is genuinely co-eval), provide a direct means of testing evolutionary predictions. Observational limits on magnetic fields within Wolf-Rayet stars are underway.

3. The role of rotation in WR stars at low metallicity is of particular interest. At present, amongst the best means of establishing rapid rotation in WR stars is by measuring departures from spherical symmetry using spectropolarimetry. This technique has been applied to bright WR stars in the Milky Way, but WR stars within the Magellanic Clouds are also within the reach of ground-based 8-10m instruments.

4. The evolutionary paths leading to WR stars and core-collapse SN remain

uncertain, as is the role played by LBV eruptions for the most massive stars. Given the observational connection between Type Ic supernovae and long-soft GRBs, do GRBs result from low metallicity massive stars undergoing chemically homogeneous evolution, massive binaries during a common envelope phase, or runaways from dense star clusters?

5. The presence of WR stars in large numbers within very low metallicity galaxies appears contrary to the expectations of single star evolutionary models neglecting rotational mixing. Are such stars exclusively produced by rapid rotation, close binary evolution, or via giant LBV eruptions?

6. Most late WC stars are known to be dust formers, the universal presence of binary companions is not yet established for all dusty WC stars. In addition, it is not clear how dust grains form within such an extreme environment, the study of which merits further study.

Acknowledgement

Thanks to Götz Gräfener, John Hillier, Norbert Langer, Georges Meynet, Tony Moffat, Nathan Smith, Dany Vanbeveren and Peredur Williams for useful comments on an early version of the manuscript. I wish to thank the Royal Society for providing financial assistance through their wonderful University Research Fellowship scheme for the past eight years.

Key Terms

Narrow-band imaging: WR candidates may be identified from narrow-band images sensitive to light from strong WR emission lines, after subtraction of images from their adjacent continua.

P Cygni profiles: Spectral lines showing blue-shifted absorption plus red-shifted emission. Characteristic of stellar outflows, associated with resonance lines of abundant ions (e.g. C IV 1548-51Å).

Non-LTE: Solution of full rate equations is necessary due to intense radiation field. Radiative processes dominate over collisional processes, so Local Thermodynamic Equilibrium (LTE) is not valid.

Radiatively driven winds: The transfer of photon momentum in the photosphere to the stellar atmosphere through absorption by (primarily) metal spectral lines.

Monte Carlo models: A statistical approach to the radiative transfer problem, using the concept of photon packets.

Clumped winds: Radiatively driven winds are intrinsically unstable, producing compressions and rarefactions in their outflows.

Collapsar: Rapidly rotating WR star undergoes core-collapse to form a black hole fed by an accretion disk, whose rotational axis collimates the gamma ray burst jet.

Gamma Ray Burst: Brief flash of gamma rays from cosmological distances. Either a merger of two neutron stars (short burst) or a collapsar (long burst).

Magnetar: Highly magnetized neutron star, observationally connected with Soft Gamma Repeaters and Anomalous X-ray Pulsars.

Reference Annotations

Gräfener & Hamann 2005: First solution of hydrodynamics within a realistic Wolf-Rayet model atmosphere.

Hillier 1989 Describes the extended atmospheric structure of a WC star.

van der Hucht 2001 Catalogue of Milky Way WR stars, including cluster membership, binarity, masses.

Lamers et al. 1991 Summary of key observational evidence in favour of a late stage of evolution for WR stars.

Massey 2003 Review article on the broader topic of massive stars within Local Group galaxies.

Meynet & Maeder 2005 Comparison between observed WR populations in galaxies with evolutionary model predictions allowing for rotational mixing.

Schaerer & Vacca 1998 Describes the determination of WR and O star populations within unresolved galaxies.

Williams et al. 1987 Describes various aspects of dust formation around WC stars.

Acronyms List

GRB Gamma Ray Burst

LBV Luminous Blue Variable

RSG Red Supergiant

WN Nitrogen sequence Wolf-Rayet

WC Carbon sequence Wolf-Rayet

WO Oxygen sequence Wolf-Rayet

LTE Local Thermodynamic Equilibrium

IMF Initial Mass Function

Side Bar

Luminous Blue Variables, also known as Hubble-Sandage or S Doradus type variables, share many characteristics of Wolf-Rayet stars. LBVs are widely believed to be the immediate progenitors of classic WN stars. LBVs possess powerful stellar winds, plus hydrogen depleted atmospheres, permitting similar analysis techniques to be used (e.g. Hillier et al. 2001). LBVs occupy a part of the Hertzsprung-Russell diagram adjacent to Wolf-Rayet stars. Typical spectral morphologies vary irregularly between A-type (at visual maximum) and B-type (at visual minimum) supergiants. Examples include AG Car and P Cyg in the Milky Way, and S Dor and R127 in the LMC (e.g. Humphreys & Davidson 1994). LBVs undergo occasional giant eruptive events – signatures of which are circumstellar nebulae – most notably undergone by η Car during two decades in the 19th Century ($\geq 10 M_{\odot}$ ejected). Giant eruptions are believed to play a major role in the evolution of very massive stars via the removal of their hydrogen-rich envelope (Davidson & Humphreys 1997; Smith et al. 2003). The origin of such huge eruptions is unclear, since line-driven radiation pressure is incapable of producing such outflows.

Literature Cited

Abbott DC, 1982. ApJ 263:723

Abbott DC, Bieging JH, Churchwell E, Torres AV. 1986. ApJ 303:239

Abbott DC, Conti PS. 1987. ARA&A 25:113

Abbott DC, Lucy LB. 1985. ApJ 288:679

Allen DA, Swings JP, Harvey PM. 1972. A&A 20:333

Anderson LS. 1989. ApJ 339:558

Asplund M, Grevesse N, Sauval AJ, Allende Prieto C, Kiselman D. 2004. A&A 417:751

Barlow MJ, Roche PF, Aitken DA. 1988. MNRAS 232:821

Barniske A, Hamann W-R, Gräfener G. 2007. In *Stellar Evolution at Low Metallicity: Mass-loss, Explosions, Cosmology*, ed. HJGLM Lamers, N Langer, T Nugis, San Francisco: ASP Conf Series 353, p.243

Bartzakos P, Moffat AFJ, Niemela VS. 2001. MNRAS 324:18

Bauer FE, Brandt WN. 2004. ApJ 601:L67

Beals CS. 1940. JRASC 34:169

Bohannan B, Crowther PA. 1999. ApJ 511:374

Bohannan B, Walborn NR. 1989. PASP 101:520

Breysacher J, Azzopardi M, Testor G. 1999. A&AS 137:117

Brown TM, Heap SR, Hubeny I, Lanz T, Lindler D. 2002. ApJ 579:L75

Cantiello M, Yoon S-C, Langer N, Livio M. 2007. A&A in press (astro-ph/0702540)

Carpano S, Pollock AMT, Wilms J, Ehle M, Schirmer M. 2007. A&A 461:L9

Castor JI, Abbott DC, Klein RI. 1975. ApJ 195:157

Chevalier RA, Li Z-Y, Fransson C. 2004. ApJ 606:369

Chu Y-H, Treffers RR, Kwitter KB. 1983. ApJS 53:937

Clark JS, Negueruela I, Crowther PA, Goodwin SP. 2005. A&A 434:949

Conti PS, 1976, In *Proc. 20th Colloq. Int. Ap. Liége,*, Liége: University of Liége, p. 193

Conti PS, Garmany CD, Massey P. 1989. ApJ 341:113

Conti PS, Garmany CD, De Loore C, Vanbeveren D. 1983. ApJ 274:302

Conti PS, Leep ME, Perry DN. 1983. ApJ 268:228

Conti PS, Massey P. 1989. ApJ 337:251

Conti PS, Massey P, Vreux J-M. 1990. ApJ 354:359

Crowther PA. 1997. MNRAS 290:L59

Crowther PA. 2000. A&A 356:191

Crowther PA. 2007. In *Stellar Evolution at Low Metallicity: Mass-loss, Explosions, Cosmology* eds. HJGLM Lamers, N Langer, T Nugis, San Francisco: ASP Conf Series 353, p.157

Crowther PA, De Marco O, Barlow MJ. 1998. MNRAS 296:367

Crowther PA, Dessart L. 1998. MNRAS 296:622

Crowther PA, Dessart L, Hillier DJ, Abbott JB, Fullerton AW. 2002. A&A 392:653

Crowther PA, Drissen L, Abbott JB, Royer P, Smartt SJ. 2003. A&A 404:483

Crowther PA, Fullerton AW, Hillier DJ, Brownsberger K, Dessart L, et al. 2000. ApJ 538:L51

Crowther PA, Hadfield LJ. 2006. A&A 449:711

Crowther PA, Hadfield LJ, Clark JS, Negueruela I, Vacca WD. 2006b. MNRAS 372, 1407

Crowther PA, Morris PW, Smith JD. 2006a. ApJ 636:1033

Crowther PA, Pasquali A, De Marco O, Schmutz W, Hillier DJ, de Koter A. 1999. A&A 350:1007

Crowther PA, Smith LJ. 1997. A&A 320:500

Crowther PA, Smith LJ, Hillier DJ. 1995b. A&A 302:457

Crowther PA, Smith LJ, Hillier DJ, Schmutz W. 1995a. A&A 293:427

Crowther PA, Smith LJ, Willis AJ. 1995c. A&A 304:269

Davidson K, Humphreys RM. 1997. ARA&A 35:1

de Koter A, Schmutz W, Lamers HJGLM. 1993. A&A 277:561

De Marco O, Schmutz W, Crowther PA, Hillier DJ, Dessart L, et al. 2000. A&A 358:187

de Mello DF, Schaerer D, Heldmann J, Leitherer C. 1998. ApJ 507:199

Dessart L, Crowther PA, Hillier DJ, Willis AJ, Morris PW, van der Hucht KA. 2000. MNRAS 315:407

Dessart L, Owocki SR. 2005. A&A 432:281

Dopita MA, Bell JF, Chu Y-H, Lozinskaya TA. 1994. ApJS 93:455

Dorfi EA, Gautschy A, Saio H. 2006. A&A 453:L35

Drew JE, Barlow MJ, Unruh YC, Parker QA, Wesson R, et al. 2004, MNRAS 351:206

Eenens PRJ, Williams PM. 1994. MNRAS 269:1082

Eichler D, Usov V. 1993. ApJ 402:271

Eldridge JJ, Vink JS. 2006. A&A 452:295

Esteban C, Smith LJ, Vilchez JM, Clegg RES. 1993. A&A 272:299

Evans CJ, Howarth ID, Irwin MJ, Burnley AW, Harries TJ. 2004. MNRAS 353:601

Figer DF. 2005. Nat 434:192

Foellmi C, Moffat AFJ, Guerrero MA. 2003a. MNRAS 338:360

Foellmi C, Moffat AFJ, Guerrero MA. 2003b. MNRAS 338:1025

Fruchter AS, Levan AJ, Strolger L, Vreeswijk PM, Thorsett SE, et al. 2006. Nat 441:463

Fryer CL, Rockefeller G, Young PA. 2006. ApJ. 647:1269

Galama TJ, Groot PJ, van Paradijs J, Kouveliotou C, Augusteijn T, et al. 1998. Nat 395:670

Gamov G. 1943. ApJ 98:500

Garnett DR, Kennicutt RCJr, Chu Y-H, Skillmann ED. 1991. PASP 103:850

Gräfener G, Hamann W-R. 2005. A&A 432:633

Gräfener G, Hamann W-R. 2007. A&A submitted

Gräfener G, Koesterke L, Hamann W-R. 2002. A&A 387:244

García-Segura G, Langer N, MacLow M-M. 1996b. A&A 316:133

García-Segura G, MacLow M-M, Langer N. 1996a. A&A 305:229

Gonzalez Delgado RM, Leitherer C, Stasinska G., Heckman TM. 2002. ApJ 580:824

Hadfield LJ, Crowther PA. 2006. MNRAS 368:1822

Hadfield LJ, Crowther PA, Schild H, Schmutz W. 2005. A&A 439:265

Hadfield LJ, Van Dyk S, Morris PW, Smith JD, Marston AP, et al. 2007. MNRAS in press (astro-ph/0612574)

Hamann W-R, Gräfener G. 2004. A&A 427:697

Hamann W-R, Gräfener G, Liermann A. 2006. A&A 457:1015

Hamann W-R, Koesterke L. 2000. A&A 360:647

Hamann W-R, Koesterke L, Wessolowski U. 1993. A&A 274:397

Hammer F, Flores H, Schaerer D, Dessauges-Zavadsky M, Le Floch́ E, Puech M. 2006. A&A 454:103

Harries TJ, Hillier DJ, Howarth ID. 1998. MNRAS 296:1072

Heger A, Langer N, Woosley SE. 2000. ApJ 528:368

Heger A, Fryer CL, Woosley SE, Langer N, Hartmann DH. 2003. ApJ 591:288

Herald JE, Hillier DJ, Schulte-Ladbeck RE. 2001. ApJ 548, 932

Hillier DJ. 1987. ApJS 63:947

Hillier DJ. 1988. ApJ 327:822

Hillier DJ. 1989. ApJ 347:392

Hillier DJ. 1991. A&A 247:455

Hillier DJ, Miller DL. 1998. ApJ 496:407

Hillier DJ, Miller DL. 1999. ApJ 519:354

Hillier DJ, Davidson K, Ishibashi K, Gull T. 2001. ApJ 553:837

Hiltner WA, Schild RE. 1966. ApJ 143:770

Hirschi R, Meynet G, Maeder A. 2005. A&A 433:1013

Hjorth J, Sollerman J, Moller P, Fynbo JPU, Woosley SE, et al. 2003. Nat 423:847

Homeier N, Blum RD, Pasquali A, Conti PS, Damineli A. 2003. A&A 408:153

Howarth ID, Schmutz W. 1992. A&A 261:503

Humphreys RM, Davidson K. 1979. ApJ 232:409

Humphreys RM, Davidson K. 1994. PASP 106:1025

Izotov YI, Foltz CB, Green RF, Guseva NG, Thuan TX. 1997. ApJ 487:L37

Kingsburgh RL, Barlow MJ. 1995. A&A 295:171

Kingsburgh RL, Barlow MJ, Storey PJ, 1995. A&A 295:75

Koesterke L, Hamann W-R. 1995. A&A 299:503

Koesterke L, Hamann W-R, Schmutz W, Wessoloski U. 1991. A&A 248:166

Kudritzki RP, Puls J. 2000. ARA&A 38:613

Kurosawa R, Hillier DJ, Pittard JM. 2002. A&A 388:957

Kurosawa R, Hillier DJ, Schulte-Ladbeck RE. 1999. AJ 118:539

Lamers HJGLM, Leitherer C. 1993. ApJ 412:771

Lamers HJGLM, Maeder A, Schmutz W, Cassinelli JP. 1991. ApJ 368:538

Lamontagne R, Moffat AFJ, Drissen L, Robert C, Matthews JM. 1996, AJ 112:2227

Langer N. 1989. A&A 220:135

Langer N. 1991. A&A 248:531

Langer N. 1998. A&A 329:551

Langer N, Hamann W-R, Lennon M, Najarro F, Pauldrach AWA, Puls J. 1994. A&A 290:819

Lefévre L, Marchenko SV, Moffat AFJ, Chené AN, Smith SR, et al. 2005. ApJ 634:L109

Leitherer C, Chapman JM, Koribalski B. 1997. ApJ 481:898

Lépine S, Moffat AFJ, St-Louis N, Marchenko SV, Dalton MJ et al. 2000, AJ 120:3201

Levesque EM, Massey P, Olsen KAG, Plez B, Josselin E, Maeder A, Meynet G. 2005. ApJ 628:973

Lucy LB, Abbott DC. 1993. ApJ 405:738

MacFadyen AI, Woosley SE. 1999. ApJ 524:262

Maeder A. 1987 A&A 178, 159

Maeder A, Meynet G. 1994. A&A 287:803

Maeder A, Meynet G. 2001. A&A 373:555

Malesani D, Tagliaferri G, Chincarini G, Della Valle M, Fugaza D, et al. 2004. ApJ 609, L5

Marchenko SV, Moffat AFJ, Crowther PA, Chené A-N, De Serres M, et al. 2004. MNRAS 353:153

Martins F, Schaerer D, Hillier DJ. 2002. A&A 382:999

Massey P. 1980. ApJ 236:526

Massey P. 1984. ApJ 281:789

Massey P. 2002. ApJS 141:81

Massey P. 2003. ARA&A 41:15

Massey P, Armandroff TE, Conti PS. 1986. AJ 92:1303

Massey P. Conti PS. 1981. ApJ 244:173

Massey P, DeGioia-Eastwood K, Waterhouse E. 2001. AJ 121:1050

Massey P, Holmes S. 2002. ApJ 580:L35

Massey P, Johnson O. 1998. ApJ 505:793

Massey P, Olsen KAG, Parker JWm. 2003. AJ 126:2362

Massey P, Parker JWm, Garmany CD. 1989. AJ 98:1305

Mazzali PA, Deng J, Tominaga N, Maeda K, Nomoto K, et al. 2003. ApJ 599:L95

Meynet G, Maeder A. 1997. A&A 321:465

Meynet G, Maeder A. 2003. A&A 404:975

Meynet G, Maeder A. 2005. A&A 429:581

Meynet G, Maeder A, Schaller G, Schaerer D, Charbonnel C. 1994. A&AS 103:97

Millour F, Petrov RG, Chesneau O, Bonneau D, Dessart L et al. 2007. A&A in press (astro-ph/0610936)

Milne EA. 1926. MNRAS 86:459

Moffat AFJ, Drissen L, Lamontagne R, Robert C. 1988. ApJ 334:1038

Moffat AFJ, Seggewiss W, Shara MM. 1985. ApJ 295:109

Moffat AFJ, Shara MM. 1987. ApJ 320:266

Mokiem MR, De Koter A, Evans CJ, Puls J, Smartt SJ et al. 2006. A&A 456:1131

Mokiem MR, De Koter A, Vink J, Puls J, Evans CJ et al. 2007. A&A submitted

Morris PM, Crowther PA, Houck JR. 2004. ApJS 154:413

Morton DC. 1967. ApJ 147:1017

Nakamura T, Mazzali PA, Nomoto K, Iwamoto K. 2001. ApJ 550:991

Nugis T, Crowther PA, Willis AJ. 1998. A&A 333:956

Nugis T, Lamers HJGLM. 2000. A&A 360:227

Nugis T, Lamers HJGLM. 2002. A&A 389:162

Owocki SR, Castor JI, Rybicki GB. 1988. ApJ 355:914

Owocki SR, Cranmer SR, Gayley KG. 1996. ApJ 472:L115

Papaderos P., Izotov YI, Guseva NG, Thuan TX, Fricke KJ. 2006. A&A 454:119

Pauldrach AWA, Puls J, Kudritzki RP. 1986. A&A 184:86

Petrovic J, Pols O, Langer N. 2006. A&A 450:219

Podskadlowski Ph, Langer N, Poelarends AJT, Rappaport S, Heger A, Pfahl E. 2004. ApJ 612:1044

Prinja RK, Barlow MJ, Howarth ID. 1990. ApJ 361:607

Rauw G, Crowther PA, De Becker M, Gosset E, Naze Y, et al. 2005. A&A 432:985

Repolust T, Puls J, Herrero A. 2004. A&A 415:349

Russell SC, Dopita MA. 1990. ApJS 74:93

Schaerer D, Maeder A. 1992. A&A 263:129

Schaerer D, Contini T, Pindao M. 1999. A&AS 136:35

Schaerer D, Vacca, WD. 1998. ApJ 497:618

Schild H, Crowther PA, Abbott JB, Schmutz W. 2003. A&A 397:859

Schild H, Güdel M, Mewe R, Schmutz W, Raassen AJJ, et al. 2004. A&A 422:177

Schild H, Maeder A. 1984. A&A 136:237

Schmutz W. 1997. A&A 321:268

Schmutz W, Hamann W-R, Wessolowski U. 1989. A&A 210:236

Schmutz W, Leitherer C, Gruenwald R. 1992. PASP 104:1164

Schweickhardt J, Schmutz W, Stahl O, Szeifert Th, Wolf B. 1999. A&A 347:127

Shapley AE, Steidel CS, Pettini M., Adelberger KL. 2003. ApJ 588:65

Skinner SL, Zhekov SA, Güdel M, Schmutz W. 2002. ApJ 579:764

Smith LF. 1968a. MNRAS 138:109

Smith LF. 1968b. MNRAS 140:409

Smith LF, Hummer DG. 1988. MNRAS 230:511

Smith LF, Maeder A. 1991. A&A 241:77

Smith LF, Shara MM, Moffat AFJ. 1996. MNRAS 281:163

Smith LJ, Crowther PA, Prinja RK. 1994. A&A 281:833

Smith LJ, Norris RPF, Crowther PA. 2002. MNRAS 337:1309

Smith LJ, Willis AJ. 1983. A&AS 54:229

Smith N, Gehrz RD, Hinz PM, Hoffmann WF, Hora JL, et al. 2003 AJ 125:1458

Smith N, Li W, Foley RJ, Wheeler JC, Pooley D, Chornock R, et al. 2007 ApJ submitted (astro-ph/0612617)

Smith N, Owocki SP. 2006. ApJ 645:L45

Sobolev VV. 1960. *Moving Envelopes of Stars*, Cambridge, Mass: Harvard University Press

Springmann U. 1994. A&A 289:505

Stahl O, Wolf B, Klare G. Cassatella A, Krautter J. et al. 1983. A&A 127:49

Stevens IR, Blondin JM, Pollock AMT. 1992. ApJ 386:265

St-Louis N, Moffat AFJ, Lapointe L, Efimov YS, Shakhovskoj NM, Fox GK, Piirola V. 1993. ApJ 410:342

St-Louis N, Chene, A-N, de la Chevrotiere A, Moffat AFJ. 2007. In *Mass loss from stars and the evolution of stellar clusters*, ed. A de Koter, LJ Smith, R Waters, San Francisco: ASP Conf Ser, in press

Torres AV, Conti PS, Massey P. 1986. ApJ 300:379

Torres-Dodgen AV, Massey P. 1988. AJ 96:1076

Townsend RHD, MacDonald J. 2006. MNRAS 368:L57

Turner DG, 1982. In *IAU Symp 99: Wolf-Rayet Stars: Observations, Physics,*

Evolution, ed. CWH de Loore, AJ Willis, Reidel: Dordrecht, p.57

Tuthill PG, Monnier JD, Danchi WC. 1999. Nat 398:487

Tuthill P, Monnier J, Tanner A, Figer D, Ghez A, Danchi W. 2006. Sci 313:935

Usov VV. 1991. MNRAS 252:49

Vacca WD, Rayner RJ, Cushing MC. 2007. ApJ to be submitted

Van Bever J., Vanbeveren D. 2003. A&A 400:63

Vanbeveren D, De Loore C, Van Rensbergen W. 1998. A&A Rev 9:63

van der Hucht KA. 2001. New A 45:135

van der Hucht KA. 2006. A&A 458, 453

van der Hucht KA, Morris PW, Williams PM, Setia Gunawan DYA. 1996. A&A 315:L193

van Kerkwijk MH, Charles PA, Geballe TR, King DL, Miley GK, et al. 1992. Nat 355:703

van Marle AJ, Langer N, García-Segura G. 2005. A&A 444:837

Villar-Sbaffi A, St-Louis N, Moffat AFJ, Piirola V. 2006. ApJ 640:995

Vink JS, de Koter A. 2005. A&A 442:587

Von Zeipel H. 1924. MNRAS 84:665

Walborn NR. 1990, in *Properties of Hot, Luminous Stars*, ed. CD. Garmany, San Francisco: ASP Conf Ser 7, p.23

Walborn NR, Morrell NI, Howarth ID, Crowther PA, Lennon DJ, et al. 2004. ApJ 608:1028

Weaver R, McCray R, Castor JI, Shapiro P, Moore R. 1977. ApJ 218:377

Wellstein S, Langer N. 1999 A&A. 350:148

Westerlund BE. 1966. ApJ 145:724

Williams PM, Dougherty SM, Davis RJ, van der Hucht KA, Bode MF, Setia

Gunawan DY. 1997. MNRAS 289:10

Williams PM, van der Hucht KA, Pollock AMT, Florkowski DR, van der Woerd H, Wamsteker WM. 1990. MNRAS 243:662

Williams PM, van der Hucht KA, Thé PS. 1987. A&A 182:91

Willis AJ, Crowther PA, Fullerton AW, Hutchings JB, Sonneborn G, et al. 2004. ApJS 154:651

Willis AJ, Schild H, Stevens IR. 1995. A&A 298:549

Willis AJ, van der Hucht KA, Conti PS, Garmany CD. 1986. A&AS 63:417

Wolf CJE, Rayet G. 1867. Comptes Rendues 65:292

Woosley SE, Bloom JS. 2006. ARA&A 44:507

Woosley SE, Heger A. 2006. ApJ 637, 914

Wright AE, Barlow MJ. 1975. MNRAS 170:41

Yoon S-C, Langer N. 2005. A&A 443:643

Zahn J-P. 1992. A&A 265:115

Table 1: Wavelength-specific observed and synthetic spectral atlases (X-ray to mid-IR) of Galactic WR stars. Predicted stellar luminosities for early-type and late-type WR stars within each spectral window are based upon the averages of HD 96548 (WR40, WN8, Herald, Hillier & Schulte-Ladbeck 2001), HD 164270 (WR103, WC9, Crowther, Morris & Smith 2006a) and HD 50896 (WR6, WN4b, Morris, Crowther & Houck 2004), HD 37026 (BAT52, WC4, Crowther et al. 2002), respectively.

λ	Window	$L_\lambda/L_{\rm bol}$		Sp Type	Reference
		Late	Early		
5–25Å	X-ray	10^{-7}	10^{-7}	WN	Skinner et al. 2002
				WC	Schild et al. 2004
<912Å	Extreme UV	39%	69%	WN, WC	Smith, Crowther & Norris 200
				WN	Hamann & Gräfener 2004
912–1200Å	Far-UV	21%	12%	WN, WC	Willis et al. 2004
1200–3200Å	UV, Near-UV	33%	16%	WN, WC	Willis et al. 1986
3200–7000Å	Visual	5%	2%	WN, WC	Conti & Massey 1989
7000–1.1μm	Far-red	0.9%	0.3%	WN, WC	Conti, Massey & Vreux 1990
				WN,WC	Howarth & Schmutz 1992
1–5μm	Near-IR	0.4%	0.2%	WN,WC	Vacca et al. 2007
5–30μm	Mid-IR	0.02%	0.01%	WN	Morris et al. 2000
				WCd	van der Hucht et al. 1996

Table 2: Physical and wind properties of Milky Way WR stars (LMC in parenthesis), adapted from Herald, Hillier & Schulte-Ladbeck (2001) and Hamann, Gräfener & Liermann (2006) for WN stars, plus Barniske, Hamann & Gräfener (2007), Crowther et al. (2002, 2006a) and references therein for WC stars. Abundances are shown by mass fraction in percent. Mass-loss rates assume a volume filling factor of f=0.1.

Sp	T_*	$\log L$	$\dot{M}$	v_∞	logN(LyC)	M_v	Example
Type	kK	$L_\odot$	$M_\odot \mathrm{yr}^{-1}$	$\mathrm{km\,s^{-1}}$	$\mathrm{ph\,s^{-1}}$	mag	
				WN stars			
3-w	85	5.34	–5.3	2200	49.2	–3.1	WR3
4-s	85	5.3	–4.9	1800	49.2	–4.0	WR6
5-w	60	5.2	–5.2	1500	49.0	–4.0	WR61
6-s	70	5.2	–4.8	1800	49.1	–4.1	WR134
7	50	5.54	–4.8	1300	49.4	–5.4	WR84
8	45	5.38	–4.7	1000	49.1	–5.5	WR40
9	32	5.7	–4.8	700	48.9	–6.7	WR105
				WNha stars			
6ha	45	6.18	–5.0	2500	49.9	–6.8	WR24
9ha	35	5.86	–4.8	1300	49.4	–7.1	WR108
				WC and WO stars			
(WO)	(150)	(5.22)	(–5.0)	(4100)	(49.0)	(–2.8)	(BAT123)
(4)	(90)	(5.54)	(–4.6)	(2750)	(49.4)	(–4.5)	(BAT52)
5	85	5.1	–4.9	2200	48.9	–3.6	WR111
6	80	5.06	–4.9	2200	48.9	–3.6	WR154
7	75	5.34	–4.7	2200	49.1	–4.5	WR90
8	65	5.14	–5.0	1700	49.0	–4.0	WR135
9	50	4.94	–5.0	1200	48.6	–4.6	WR103

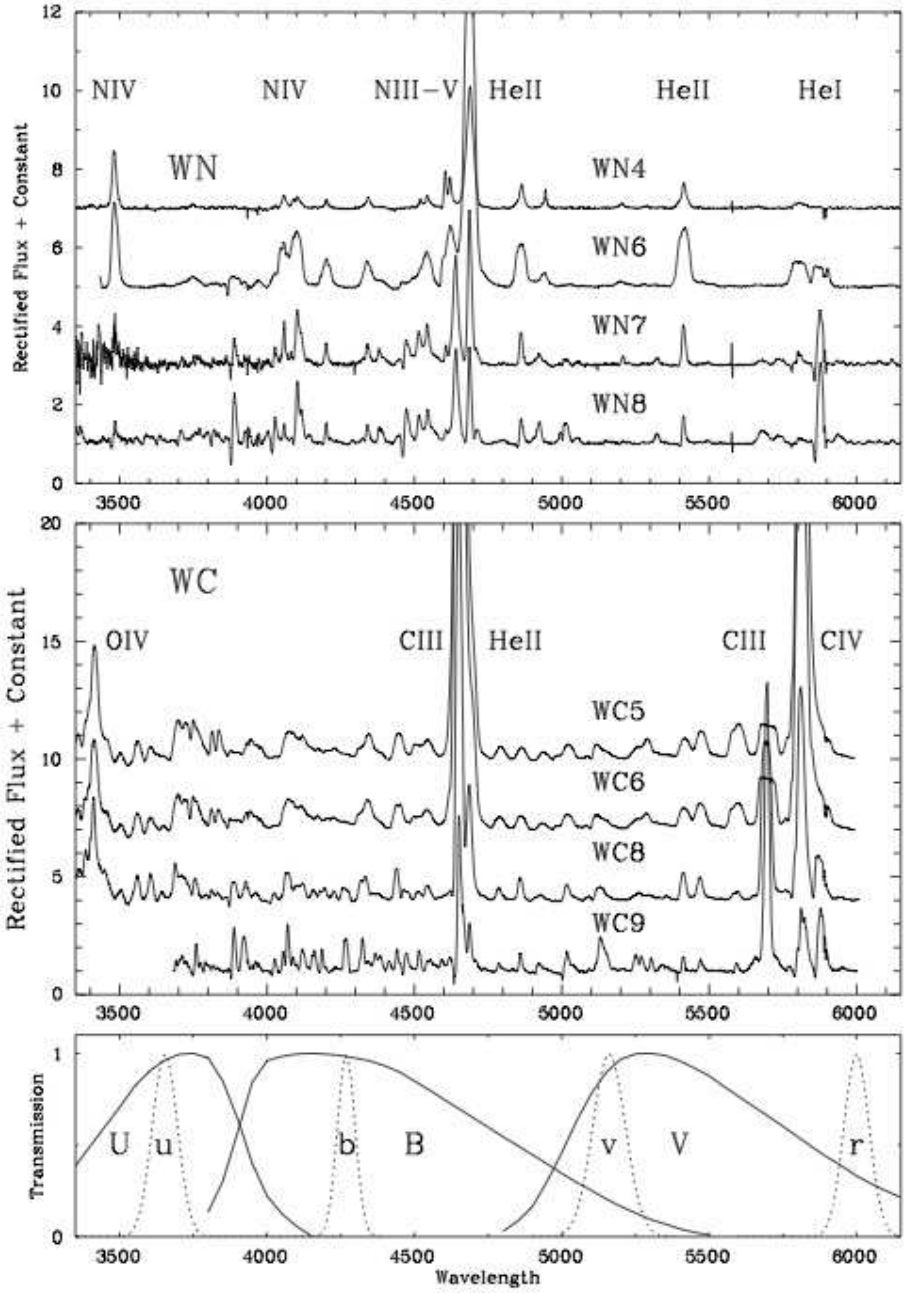

Figure 1: Montage of optical spectroscopy of Milky Way WN and WC stars together with the Smith (1968b) *ubv* and Massey (1984) *r* narrow-band and Johnson UBV broad-band filters

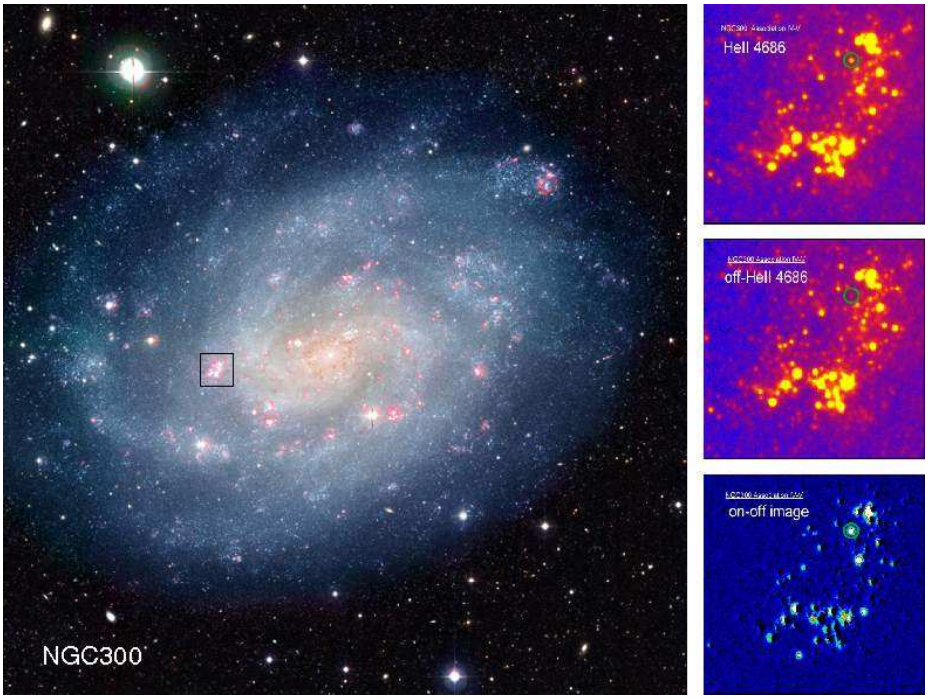

Figure 2: Composite ESO Wide Field Imager B, V, R and Hα image of NGC 300 obtained at the MPG/ESO 2.2m telescope (Press Photo 18a-h/02). A box marks the OB association IV-V (40×40 arcsec). Narrow-band images of the association are shown on the right, centred at λ4684 (He II 4686, top) and λ4781 (off-He II 4686, middle), plus a difference image (on-off, bottom) obtained with ESO VLT/FORS2 (Schild et al. 2003). A number of WR stars showing a He II excess (white) can be seen in the lower right image, including a WC4 star (green circle in all FORS2 images).

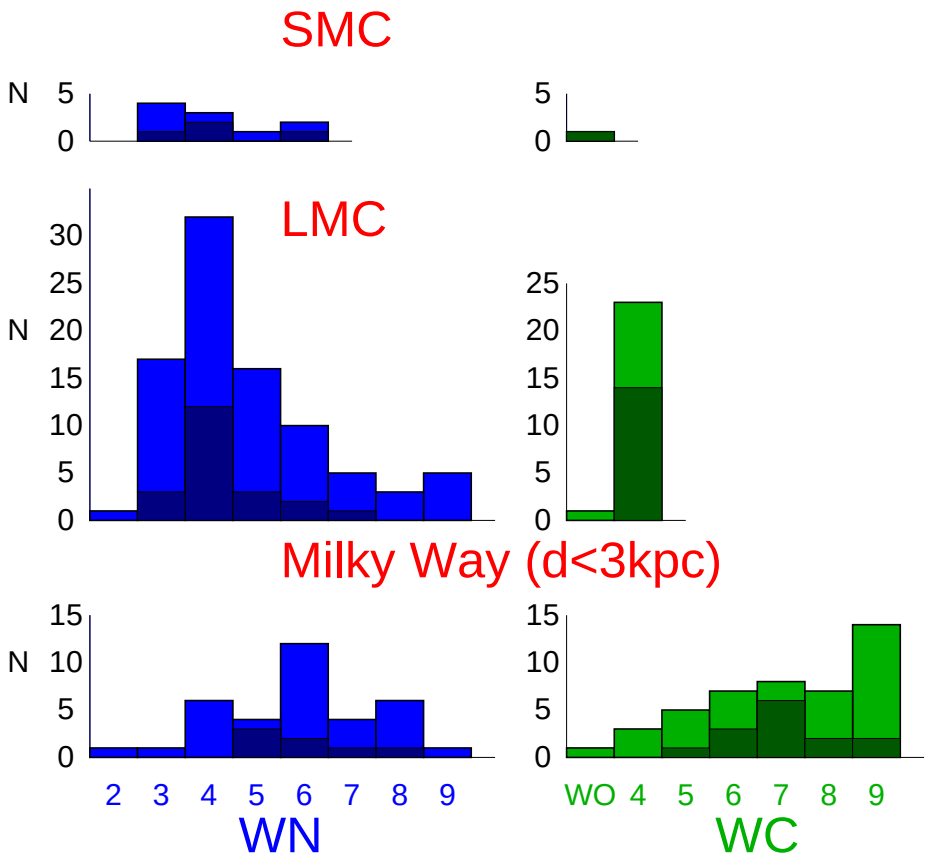

Figure 3: Subtype distribution of Milky Way (d <3kpc), LMC, and SMC WR stars, according to van der Hucht (2001), Bartzakos, Moffat & Niemela (2001), Foellmi, Moffat & Guerrero (2003ab). Both visual and close WR binaries are shaded (e.g. only 3 of the LMC WC4 stars are close binaries according to Bartzakos et al. 2001). Rare, intermediate WN/C stars are included in the WN sample.

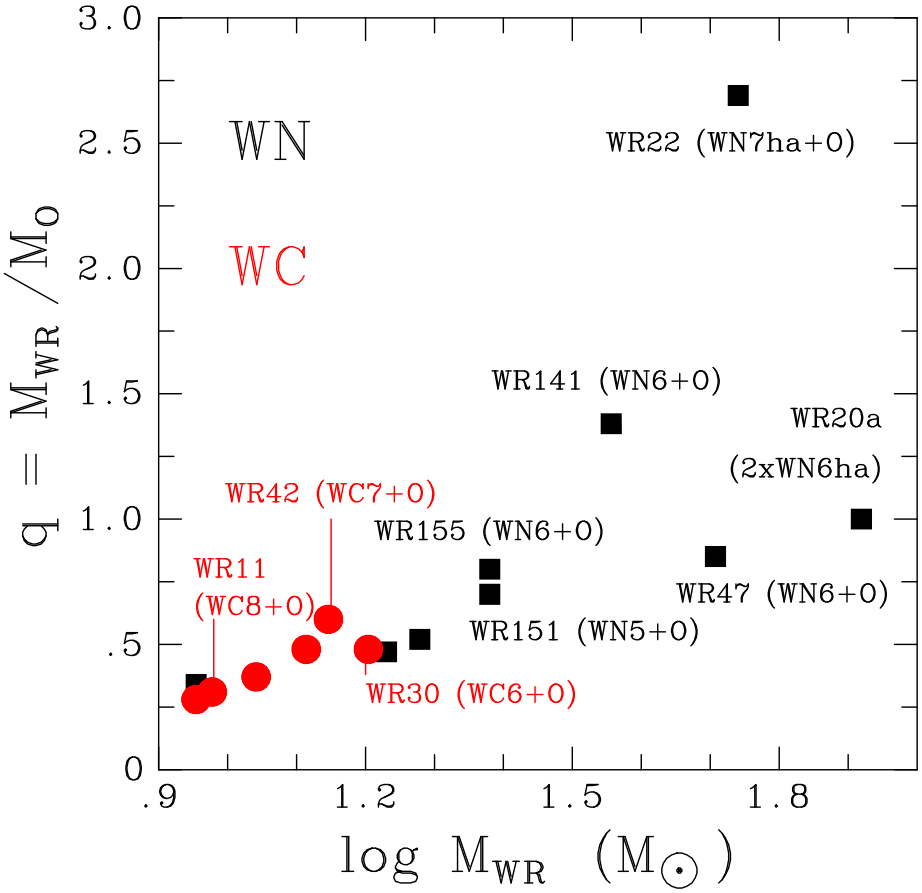

Figure 4: Stellar masses for Milky Way WR stars obtained from binary orbits (van der Hucht 2001; Rauw et al. 2005; Villar-Sbaffi et al. 2006)

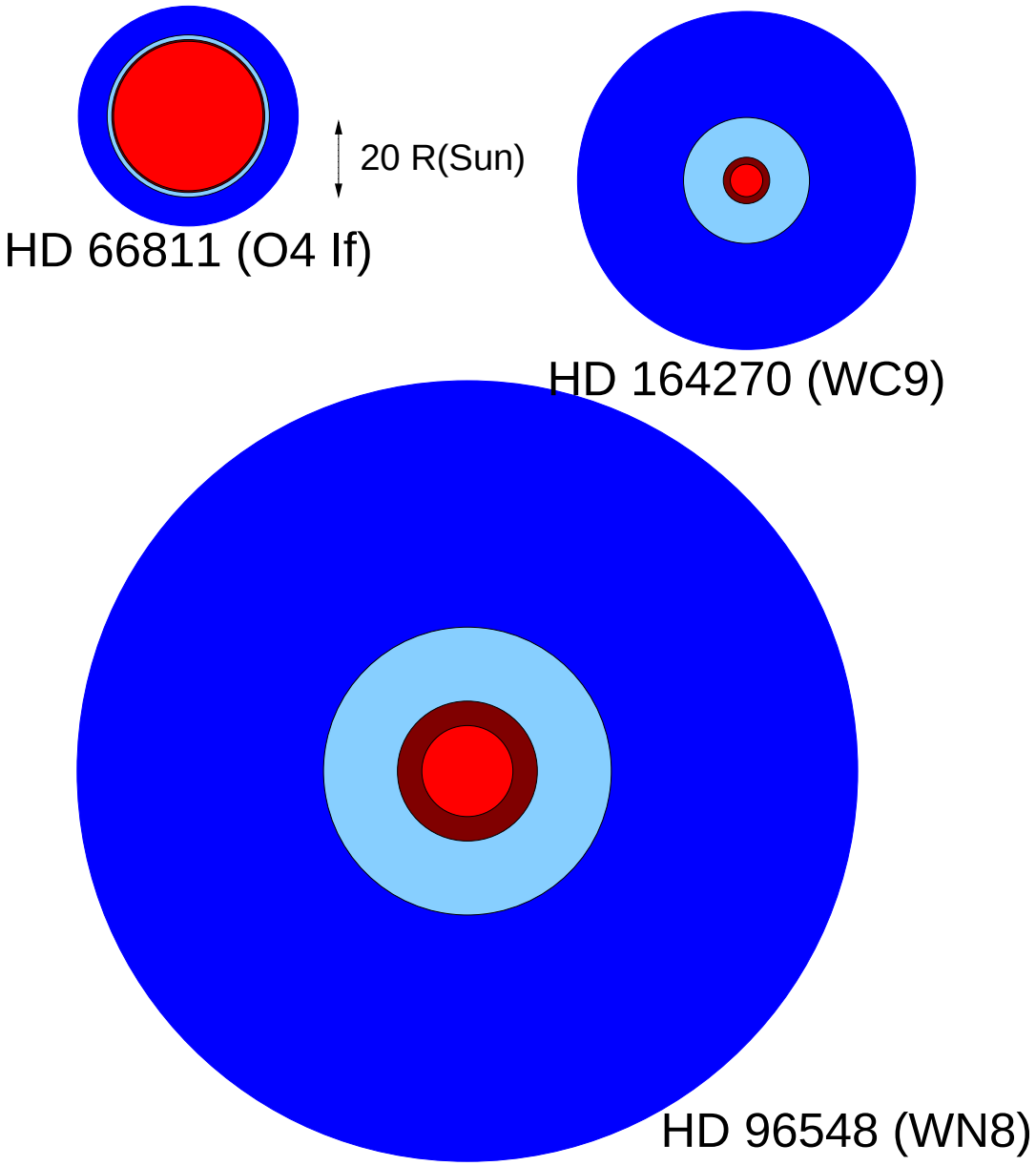

Figure 5: Comparisons between stellar radii at Rosseland optical depths of 20 (= R_*, red) and 2/3 (= $R_{2/3}$, dark red) for HD 66811 (O4 If), HD 96548 (WR40, WN8) and HD 164270 (WR103, WC9), shown to scale. The primary optical wind line-forming region, $10^{11} \leq n_e \leq 10^{12}$ cm^{-3} is shown in dark blue, plus higher density wind material, $n_e \geq 10^{12}$ cm^{-3} is indicated in light blue. The figure illustrates the highly extended winds of WR stars with respect to O stars (Repolust, Puls & Herrero 2004; Herald, Hillier & Schulte-Ladbeck 2001; Crowther, Morris & Smith 2006a).

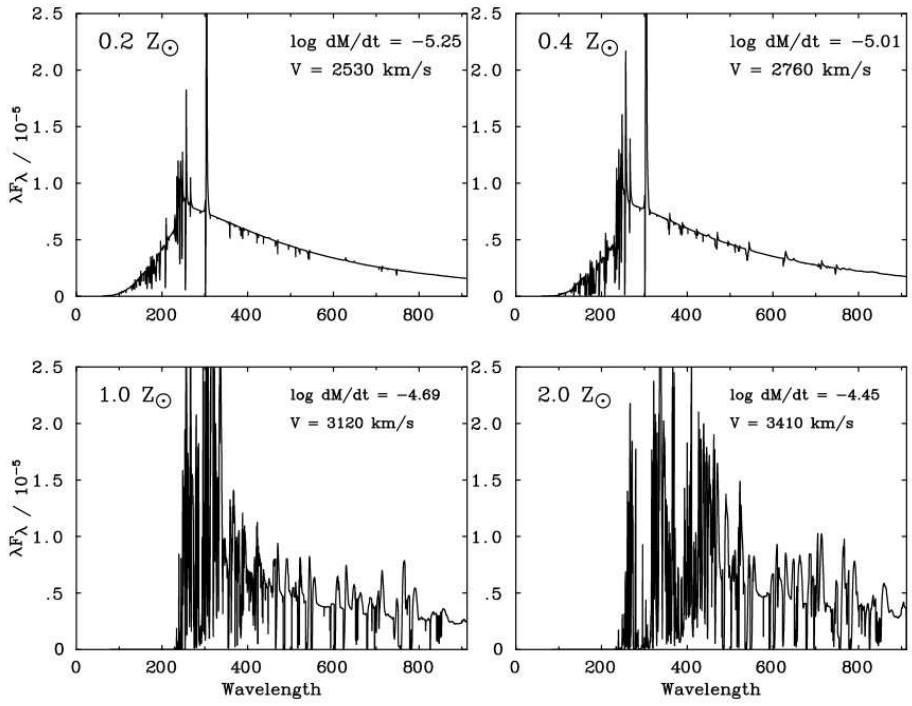

Figure 6: Comparison between the Lyman continuum ionizing fluxes of early WN CMFGEN models with fixed parameters (100 kK, $\log L/L_{\odot} = 5.48$), except that the mass-loss rates and wind velocities depend upon metallicities according to Smith, Norris & Crowther (2002). Only the low wind density models predict a significant flux below the He^{+} edge at 228Å

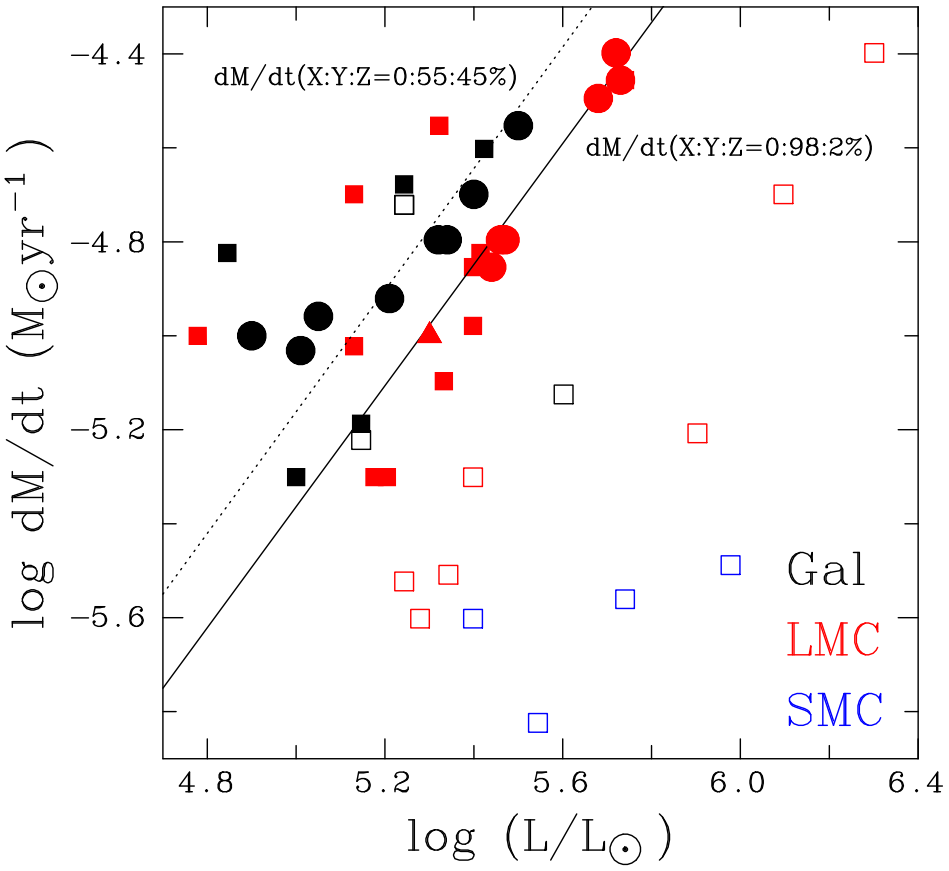

Figure 7: Comparison between the mass-loss rates and luminosities of WN3–6 (squares), WC5–9 (circles) and WO (triangles) stars in the Galaxy (black), LMC (red) and SMC (blue). Eqn 6 from Nugis & Lamers (2000) for H-poor WN (solid line) and WC stars (dotted line) is included. Open/filled symbols refer to WN stars with/without surface hydrogen, based upon analysis of near-IR helium lines (Crowther 2007). Mass-loss rates are universally high if hydrogen is absent.

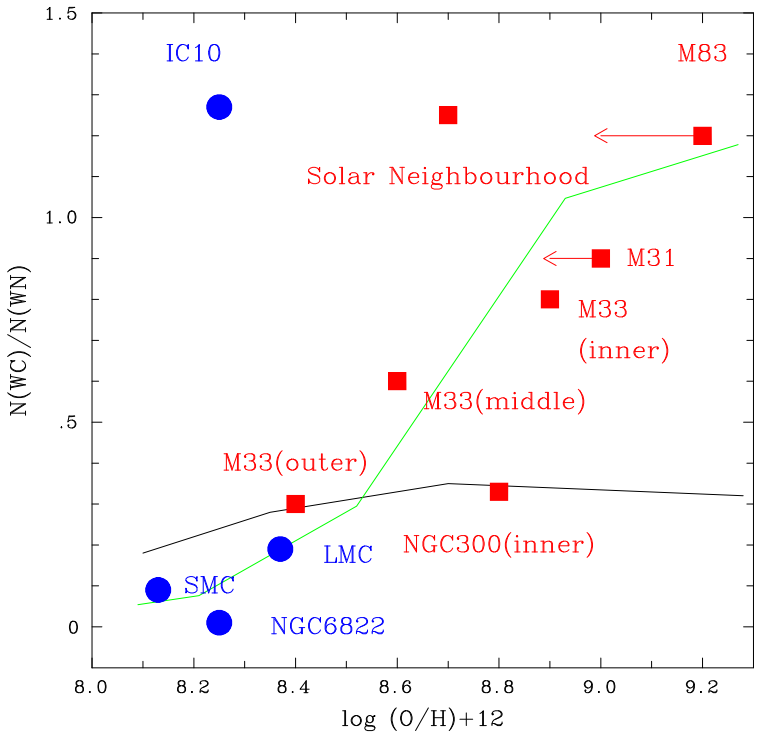

Figure 8: Comparison between observed N(WC)/N(WN) ratio and oxygen content, for nearby spiral (red) and irregular (blue) galaxies (Massey & Johnson 1998; Crowther et al. 2003; Schild et al. 2003; Hadfield et al. 2005) together with evolutionary model predictions by Meynet & Maeder (2005, black) and Eldridge & Vink (2006, green). Different regions of M33 are shown (inner, middle, outer), resulting from the strong metallicity gradient in that galaxy.